

Submitted to *The Astrophysical Journal*

## Electric Dipole Radiation from Spinning Dust Grains

B.T. Draine & A. Lazarian

Princeton University Observatory, Peyton Hall, Princeton, NJ 08544

### ABSTRACT

We discuss the rotational excitation of small interstellar grains and the resulting electric dipole radiation from spinning dust. Attention is given to excitation and damping of grain rotation by: collisions with neutrals; collisions with ions; “plasma drag”; emission of infrared radiation; emission of electric dipole radiation; photoelectric emission; and formation of H<sub>2</sub> on the grain surface. Electrostatic “focussing” can substantially enhance the rate of rotational excitation of grains colliding with ions. Under some conditions, “plasma drag” – due to interaction of the electric dipole moment of the grain with the electric field produced by passing ions – dominates both rotational damping and rotational excitation. We introduce dimensionless functions  $F$  and  $G$  which allow direct comparison of the contributions of different mechanisms to rotational drag and excitation.

Emissivities are estimated for dust in different phases of the interstellar medium, including diffuse HI clouds, warm HI, low-density photoionized gas, and cold molecular gas. Spinning dust grains could explain much, and perhaps all, of the 14 - 50 GHz background component recently observed by Kogut et al. (1996), de Oliveira-Costa et al. (1997) and Leitch et al. (1997). Future sensitive measurements of angular structure in the microwave sky brightness from the ground and from space should detect this emission from high-latitude HI clouds. It should be possible to detect rotational emission from small grains by ground-based pointed observations of molecular clouds.

*Subject headings:* ISM: Atomic Processes, Dust, Radiation; Cosmic Microwave Background

## 1. Introduction

Experiments to map the cosmic microwave background radiation have stimulated renewed interest in diffuse Galactic emission. Most recently, Kogut et al (1996), de Oliveira-Costa et al. (1997) and Leitch et al. (1997) have reported a new component of galactic microwave emission which is correlated with  $100\mu\text{m}$  thermal emission from interstellar dust.

Kogut et al. found the emission excess to have  $I_\nu(31.5\text{GHz}) \approx I_\nu(53\text{GHz})$ , and Leitch et al. found  $I_\nu(14.5\text{GHz}) \approx I_\nu(32\text{GHz})$ , consistent with the spectrum of free-free emission, but nondetection of  $\text{H}\alpha$  emission in these directions is inconsistent with free-free emission accounting for the microwave excess unless the plasma temperature  $T \gtrsim 10^6\text{K}$ . Leitch et al. therefore proposed that the observed emission was free-free emission from shock-heated gas in a supernova remnant.

Draine & Lazarian (1998, hereafter DL98) showed, however, that the observed microwave excess could not be due to free-free emission from hot gas, as this would require an energy injection rate at least 2 orders of magnitude greater than that the energy input due to supernovae. DL98 showed that the microwave excess could in fact be electric dipole emission from rapidly-rotating dust grains.

To predict the intensity of dipole emission one needs (1) the numbers of small grains, (2) their dipole moments, and (3) their rotational velocities. The observed intensity of 12 and  $25\mu\text{m}$  emission from interstellar clouds allows us to estimate the numbers of very small grains (Leger & Puget 1984; Draine & Anderson 1985; Desert, Boulanger, & Puget 1990). To estimate the dipole moments, we consider the likely displacements between the charge and mass centroids for grains, plus the intrinsic dipole moment arising from polarized chemical bonds in the grain material. However, the main thrust of the present paper is a comprehensive study of the rotational dynamics of small grains, in order to estimate their rotation rates.

Ferrara & Dettmar (1994) showed that small grains rotating with thermal rotation rates could produce detectable radio emission, but they did not address the details of rotational excitation and damping. Rotational excitation of small grains (= large molecules) has been discussed previously by Rouan et al (1992), who described the effects of collisions with gas atoms and absorption and emission of radiation. In the present work we reexamine this problem, and include the important effects of collisions with ions, which were neglected in the study by Rouan et al. We also include the effects of “plasma drag” due to interaction of the grain with passing ions, first considered by Anderson & Watson (1993). We derive rates for rotational damping and excitation due to plasma drag which are somewhat larger

than estimated by Anderson & Watson (1993).

We discuss rotational excitation as a function of both grain size and environmental conditions. Electrostatic focussing of ions makes them very effective at delivering angular momentum to the grains; ion collisions can dominate the rotational excitation of very small grains even in predominantly neutral regions.

For our adopted population of very small grains, we predict the microwave emissivity of various phases of the interstellar medium, ranging from diffuse gas to molecular clouds. We expect detectable levels of emission from spinning dust grains in all of these phases.

The paper is organized as follows: After describing the environments which we consider (§2), we discuss the electric dipole moments expected for small dust grains (§3). The various rotational damping processes are reviewed in §4, and the rotational excitation mechanisms in §5. Using these rates for rotational excitation and damping, we calculate the resulting rate of grain rotation in §6. The importance of the impulsive nature of the rotational excitation is discussed in §7, and the effects of centrifugal stresses in §8.

The reader interested primarily in the predicted emission may wish to skip §§2–8 and proceed directly to §9, where we describe our assumptions concerning the grain size distribution in various environments. We present the microwave emission spectra expected for grains in both diffuse regions and molecular clouds in §10. The detection of this microwave emission from pointed observations of dense clouds is discussed in §11. The principal uncertainties in our estimates are discussed in §12, and our results are summarized in §13.

## 2. Environments

We will consider grains in five different idealized “phases” of the interstellar medium: “Cold Neutral Medium” (CNM), “Warm Neutral Medium” (WNM), “Warm Ionized Medium” (WIM), “Molecular Cloud” (MC), and “Dark Cloud” (DC). In Table 1 we give the adopted values of  $n_{\text{H}}$  (H nucleon density),  $T$  (gas kinetic temperature),  $\chi$  (starlight intensity relative to the average starlight background), and other properties of these phases.

## 3. Grain Properties

### 3.1. Grain Sizes and Shapes

We will characterize the grain size by the “volume equivalent” radius  $a \equiv 10^{-7}a_{-7}$  cm, the radius of a sphere of equal volume. We will assume a density  $\rho \approx 2. \text{ g cm}^{-3}$ , having in mind a carbonaceous material with C:H $\approx$ 3:1; for C:H::3:1 the mass per atom is  $m \approx 9.25$  amu, and the number of atoms in the grain is then

$$N = 545a_{-7}^3 \quad . \quad (1)$$

We will consider grains down to a minimum size  $N \approx 25$ , or  $a_{-7} \approx 0.36$ .

We require the moment of inertia as a function of grain size, so assumptions must be made concerning the grain shape. The smallest grains may be chainlike, as favored by Thaddeus (1995), or sheetlike, as expected for polycyclic aromatic hydrocarbons. For generality, we will suppose that grains with  $a < a_1$  are cylindrical with diameter  $d$ , grains with  $a_1 < a < a_2$  are disklike with thickness  $d$ , and grains with  $a > a_2$  are spherical; we take  $d = 3.35 \times 10^{-8}$  cm, the interlayer separation in graphite. The actual geometry of small grains is uncertain. Here we usually take  $a_1 = 0$  and  $a_2 = 6 \times 10^{-8}$  cm (grains with  $N < 120$  atoms are disklike), but we will also consider the possibility that  $a_1 = 4 \times 10^{-8}$  cm (grains with  $N < 50$  atoms are linear).

The physics of rotational excitation and damping will be explicitly derived for spherical grains; when nonspherical grains are considered, we will attempt to use results for spherical grains but with the radius  $a$  for the sphere replaced by an appropriate length scale for the nonspherical shape. For convex shapes, the rates for collisions of neutral grains with atoms depends on the surface area  $S$ , and we therefore define the “surface-equivalent” radius  $a_s$ , the radius of a sphere with equal surface area:

$$4\pi a_s^2 \equiv S \quad . \quad (2)$$

The excitation of rotational kinetic energy by collisions is proportional to  $\int r^2 dS$ , where  $r$  is the distance from the surface point to the center-of-mass. We therefore define the “excitation equivalent” radius  $a_x$ , the radius of a sphere with equal  $\int r^2 dS$ :

$$4\pi a_x^4 \equiv \int r^2 dS \quad . \quad (3)$$

Another important quantity is the ratio of the moment of inertia to the value for a sphere of radius  $a$ :  $\xi \equiv I/(0.4Ma^2)$ , where  $M$  is the grain mass and  $I$  is the largest eigenvalue of the moment of inertia tensor.

### 3.2. Grain Charge

Grains acquire charge through photoelectric emission and collisions with electrons and ions. Bakes & Tielens (1994) have discussed the rate  $\dot{N}_{pe}(Z)$  of photoelectron emission from a carbonaceous particle with charge  $Ze$ ; we adopt their rates with minor modifications (Weingartner & Draine 1998). Collisional charging processes have been discussed by Draine & Sutin (1987), whose rates we employ here. When considering nonspherical grains, we approximate the potential as  $U \approx Ze/a_s$ . In computing the electron and ion capture rates, we assume a spherical geometry with a radius  $a_s$ .

Let  $\dot{N}_e(Z)$  and  $\dot{N}_i(Z)$  be the rate of electron capture and ion impact for a grain of radius  $a_s$  and charge  $Ze$ . With these rates, we solve the usual equations to obtain the steady-state charge distribution function  $f(Z)$  for grains of radius  $a$ :

$$\left[ \dot{N}_i(Z) + \dot{N}_{pe}(Z) \right] f(Z) = \dot{N}_e(Z+1)f(Z+1) \quad . \quad (4)$$

Selected charge distribution functions  $f(Z)$  are shown in Figure 1 for CNM and WNM conditions.

The charge distribution for grains of radius  $a$  has mode  $Z_m$ , centroid  $\langle Z \rangle$ , and variance  $\sigma_Z^2 = \langle Z^2 \rangle - \langle Z \rangle^2$ ; these are shown in Figure 2. The time scale for changes in the grain charge is of interest. We define a characteristic charging time by

$$\tau_Z = \frac{1 + \sigma_Z^2}{\dot{N}_e(Z_m) + \dot{N}_i(Z_m) + \dot{N}_{pe}(Z_m)} \quad (5)$$

When  $\sigma_Z^2 \ll 1$ ,  $\tau_Z$  is simply the lifetime of charge state  $Z_m$ ; when  $\sigma_Z^2 \gg 1$ ,  $\tau_Z$  is an estimate for the time required for the grain charge to change by of order the standard deviation  $\sigma_Z$  of the charge distribution.

Figure 3 shows  $\tau_Z$  as a function of grain size  $a$  for CNM and WNM conditions.

### 3.3. Quantum vs. Classical Dynamics

The grain angular momentum  $I\omega$  is quantized. If the rotational kinetic energy is  $(3/2)kT_{rot}$ , then the rotational quantum number

$$J = \frac{I\omega}{\hbar} = 5.85\xi^{1/2}N^{5/6} \left( \frac{T_{rot}}{100\text{K}} \right)^{1/2} \quad . \quad (6)$$

The smallest grain we consider will have  $\xi^{3/5}N \gtrsim 35$ , so that  $J \gtrsim 113(T_{rot}/100\text{K})^{1/2} \gg 1$ . We are therefore justified in using classical mechanics to discuss the grain rotation.

### 3.4. Grain Dipole Moments

A spinning grain radiates power

$$P = \frac{2\omega^4\mu^2\sin^2\theta}{3c^3} \quad , \quad (7)$$

where  $\theta$  is the angle between the angular velocity  $\omega$  and electric dipole moment  $\mu$ . We assume that the grain dipole moment  $\mu$  can be written

$$\mu = \mu_i + \epsilon Zea_x \quad , \quad (8)$$

where  $\mu_i$  is the intrinsic dipole moment of an uncharged grain,  $Ze$  is the grain charge, and the vector  $\epsilon a_x$  is the displacement between the grain center of mass and the charge centroid [the length  $a_x$  is defined by eq.(3)]. As noted by Purcell (1976), an irregular grain, even if perfectly conducting, will, in general, have its charge centroid displaced from the mass centroid. The magnitude of the displacement depends on the grain shape; we will assume it to be  $\sim 10\%$  of  $a_x$ , or  $|\epsilon| \approx 0.1$ . Thus

$$\epsilon Zea_x = 4.8 \left( \frac{a_x}{10^{-7} \text{ cm}} \right) Z \left( \frac{|\epsilon|}{0.1} \right) \text{ debye} \quad . \quad (9)$$

Neutral molecules can of course have electric dipole moments. Except for the case of highly symmetric molecules, these dipole moments are expected to be appreciable. If the grain material has short range order, but minimal long-range order, then it consists of more-or-less randomly-arranged chemical substructures, and

$$\mu_i \approx N^{1/2}\beta \quad . \quad (10)$$

To estimate the likely magnitude of  $\beta$ , we show in Table 2 the dipole moments associated with particular bonds in hydrocarbon molecules. Dipole moments of  $\sim 1$  debye are evidently typical in hydrocarbon molecules. Of course, a highly symmetric molecule would have a net dipole moment of zero, but we do not expect such perfect symmetry to be the norm for large interstellar molecules. The larger molecules should have minimal long-range order, having grown by random arrival of gas atoms or by coagulation with other small molecules. It might be argued that very small molecules will be predominantly symmetric because only the most robust molecules will survive in the interstellar ultraviolet radiation field. For example, the highly symmetric polycyclic aromatic hydrocarbon  $C_{24}H_{12}$  coronene (with  $\mu_i = 0$ ) has been considered as a candidate for the very smallest interstellar grains. We note, however, that under interstellar conditions the carbon skeleton for very small grains is expected not to be fully hydrogenated (Omont 1986). Such radicals are not easily studied

in the laboratory, and dipole moments are unavailable. We can estimate, however, that substitution of OH for one of the H in coronene would produce a molecule with a dipole moment of  $\sim 1.6$  debye, or  $\beta \approx 0.3$  debye. In Table 3 we give electric dipole moments for selected molecules, as well as the corresponding values of  $\beta = \mu_i/N^{0.5}$ .

Based on Table 3, and the expectation that radicals will typically have larger dipole moments than complete molecules, we will take  $\beta_0 = 0.4$  debye as representative.<sup>1</sup>

In an ensemble of grains of radius  $a$ , we may suppose the direction of  $\epsilon$  and the direction of the grain’s intrinsic dipole moment  $\mu_i$  to be uncorrelated. Thus, with  $\epsilon = 0.1$  and  $\beta = 0.4$  debye the mean square dipole moment will be

$$\mu^2 = [(4.8)^2 \left(\frac{a_x}{a}\right)^2 \langle Z^2 \rangle + (9.3)^2 a_{-7}] a_{-7}^2 (\text{debye})^2 \quad . \quad (11)$$

If the orientation of  $\mu$  is uncorrelated with the angular velocity  $\omega$ , then  $\langle \sin^2 \theta \rangle = 2/3$ , and the expected radiated power per grain is just

$$P = \frac{4}{9} \frac{\mu^2 \omega^4}{c^3} \quad . \quad (12)$$

#### 4. Rotational Damping

Gas-grain interactions, plasma-grain interactions, infrared emission, and radio emission damp the rotation of small grains. In this section we present the rates for these processes.

We consider a spherical grain with temperature  $T_d$  in gas of temperature  $T$ , H nucleon density  $n_H = n(\text{H}) + 2n(\text{H}_2)$ , and with  $n(\text{He}) = 0.1n_H$ .

In thermal equilibrium at temperature  $T$ , the grain would have an rms rotation frequency

$$\frac{\omega_T}{2\pi} = \langle \nu^2 \rangle^{1/2} \approx 5.60 \times 10^9 a_{-7}^{-5/2} \xi^{-1/2} T_2^{1/2} \quad \text{Hz} \quad , \quad (13)$$

where  $T_2 = T/100\text{K}$ . If the dust temperature  $T_d \neq T$ , or there are sources of rotational excitation and drag other than the gas (see below), then the grain rotation rate will differ from eq.(13).

Here we summarize the contributions of gas-grain interactions to both rotational damping and excitation; details may be found in Appendix B. It is convenient to “normalize” the various drag processes to the drag which would be produced by “sticky”

---

<sup>1</sup> Rouan et al. (1992) assumed  $\mu = 3$  debye for  $N = 90$ , or  $\beta = 0.32$  debye.

collisions in a pure H gas of density  $n_{\text{H}}$ : thus for drag process  $j$  we define the dimensionless quantity  $F_j$  such that the contribution of process  $j$  to the drag torque is

$$I \left( \frac{d\omega}{dt} \right)_j \equiv - \left[ n_{\text{H}} \left( \frac{8kT}{\pi m_{\text{H}}} \right)^{1/2} \frac{2\pi a_x^4 m_{\text{H}}}{3} \right] \omega F_j \quad . \quad (14)$$

Neutral grains in a gas of pure H atoms would have  $F = 1$ , with a rotational damping time

$$\tau_{\text{H}} = \frac{4\xi\rho a^5}{5n_{\text{H}}m_{\text{H}}a_x^4} \left( \frac{\pi m_{\text{H}}}{8kT} \right)^{1/2} \quad (15)$$

$$= 3.30 \times 10^{10} \xi \left( \frac{20 \text{ cm}^{-3}}{n_{\text{H}}} \right) T_2^{-1/2} a_{-7} \left( \frac{a}{a_x} \right)^4 \text{ s} \quad , \quad (16)$$

where we have assumed  $\rho = 2 \text{ g cm}^{-3}$ . We will use  $\tau_{\text{H}}$  as a fiducial time scale for the different sources of rotational damping. Thus the rotational damping time due to process  $j$  is

$$\tau_j^{-1} = F_j \tau_{\text{H}}^{-1} \quad . \quad (17)$$

The linear drag processes are additive:

$$F = F_n + F_i + F_p + F_{\text{IR}} \quad , \quad (18)$$

where  $F_n$ ,  $F_i$ ,  $F_p$ , and  $F_{\text{IR}}$  are the contributions from neutral impacts, ion impacts, plasma drag, and thermal emission of infrared photons.

#### 4.1. Collisional Drag

Collisional damping is a well-studied process (see Jones & Spitzer 1967). We assume that when species (e.g., H, H<sub>2</sub>, He) arrive at the grain surface they temporarily “stick” and then are desorbed with a thermal velocity distribution relative to the local (moving) grain surface (the possible effects of H<sub>2</sub> formation are considered separately in §5.6). The dimensionless factor  $F_j$  for species  $j$ , which would be unity for H atoms and neutral grains, depends on the grain radius  $a$ , charge state  $Z_g$ , and on the gas composition and temperature  $T$ .

Let  $f(Z_g)$  be the probability that the grain will have a charge  $Z_g e$ . Because the charging timescale  $\tau_Z$  is short compared to the timescale  $\tau_J$  over which the grain rotation rate changes appreciably, we can average over the grain charge distribution  $f(Z_g)$ . Then



(cf. Appendix B.2 and B.3)<sup>2</sup>

$$F_n = \sum_{Z_g} f(Z_g) \sum_n \frac{n_n}{n_H} \left( \frac{m_n}{m_H} \right)^{1/2} \left[ \exp(-Z_g^2 \epsilon_n^2) + |Z_g| \epsilon_n \pi^{1/2} \operatorname{erf}(|Z_g| \epsilon_n) \right] \quad , \quad (19)$$

$$F_i = \sum_{Z_g \neq 0} f(Z_g) \sum_i \frac{n_i}{n_H} \left( \frac{m_i}{m_H} \right)^{1/2} g_1 \left( \frac{Z_g Z_i e^2}{a_s k T} \right) + f(Z_g = 0) \sum_i \frac{n_i}{n_H} \left( \frac{m_i}{m_H} \right)^{1/2} \left( 1 + \frac{\pi^{1/2}}{2} Z_i \phi \right) \quad , \quad (20)$$

$$(21)$$

where

$$g_1(x) = \begin{cases} 1 - x & \text{if } x < 0 \\ e^{-x} & \text{if } x > 0 \end{cases} \quad , \quad (22)$$

$$\epsilon_n^2 \equiv \frac{e^2 \alpha_n}{2 a_s^4 k T} \quad , \quad (23)$$

$$\phi = \left( \frac{2e^2}{a_s k T} \right)^{1/2} \quad , \quad (24)$$

$n_n$ ,  $m_n$  and  $\alpha_n$  are the number density, mass, and polarizability of neutral species  $n$ . Equation (19) requires summation over neutral species  $n$ , and eq. (20) over ion species  $i$ .  $F_n$  and  $F_i$  are shown in Figs. 4 – 7 for MC, CNM, WNM, and WIM conditions.

## 4.2. Plasma Drag

If the grain has an electric dipole moment  $\mu$ , then the interaction of this electric dipole moment with passing ions couples the grain rotation to the plasma (Anderson & Watson 1993). The contribution to the damping is derived in Appendix B.4<sup>3</sup>

$$F_p \approx \frac{2e^2 \mu^2}{3a_x^4 (kT)^2} \sum_i \frac{n_i Z_i^2}{n_H} \left( \frac{m_i}{m_H} \right)^{1/2} \left\{ \ln(b_\omega/a) + \cos^2 \Psi \ln [\min(b_q, \lambda_D/b_\omega)] \right\} \quad , \quad (25)$$

where

$$\lambda_D \equiv \left( \frac{kT}{4\pi n_e e^2} \right)^{1/2} \quad (26)$$

---

<sup>2</sup> For nonspherical grains we use the length scale  $a_s$  to estimate the potential  $\sim Ze/a_s$  and surface electric field  $\sim Ze/a_s^2$ .

<sup>3</sup> In eq.(25) the factor  $a_x^{-4}$  enters because of the normalization (14).

is the Debye shielding length,

$$b_\omega = (I/m)^{1/2} \quad , \quad (27)$$

$$b_q = I(2kT/m_i)^{1/2}/\hbar \quad (28)$$

and  $\Psi$  is the angle between  $\boldsymbol{\mu}$  and  $\boldsymbol{\omega}$ . Our result (25) differs from that of Anderson & Watson (1993), who neglect impact parameters with  $b > b_\omega$ . In the present calculations we set  $\cos^2 \Psi = 1/3$ , appropriate if  $\boldsymbol{\omega}$  is randomly oriented relative to  $\boldsymbol{\mu}$ .<sup>4</sup>  $F_p$  is shown in Figs. 4 – 7.

### 4.3. Infrared Emission

A more subtle process is damping due to infrared emission (Purcell & Spitzer 1971; Martin 1972). As shown in Appendix C, emission of a thermally-excited photon of energy  $h\nu$  from a spherical grain rotating at angular velocity  $\omega \ll \nu$  removes, on average, an angular momentum  $\hbar\omega/(2\pi\nu)$ . The grain is heated by absorption of photons from the background starlight, with energy density  $u_*$ , which we assume to have the spectrum estimated for interstellar starlight by Mezger, Mathis, & Panagia (1982) and Mathis, Mezger, & Panagia (1983). The infrared emission cross section is assumed to scale with frequency as

$$Q_\nu = Q_0 \left( \frac{\nu}{\nu_0} \right)^2 \quad , \quad (29)$$

as appropriate for graphite, silicate, and various other candidate grain materials (Draine & Lee 1984). Since there is reason to believe that the smallest interstellar grains are predominantly carbonaceous,<sup>5</sup> here we will assume optical properties appropriate for small graphitic particles (though the discussion in Appendix C is fully general).

If the grain is large enough that its temperature may be approximated as a constant  $T_d$ , then the rotational drag is characterized by (see Appendix C.1)<sup>6</sup>

$$F_{\text{IR},c} = \frac{60.8}{a_{-7}} \left( \frac{u_*}{u_{\text{ISRF}}} \right)^{2/3} \left( \frac{20 \text{ cm}^{-3}}{n_{\text{H}}} \right) \left( \frac{100\text{K}}{T} \right)^{1/2} \left( \frac{a}{a_x} \right)^4 \quad . \quad (30)$$

<sup>4</sup> We note, however, that disklike grains would tend to have  $\cos^2 \Psi \approx 1$ , since internal relaxation will cause the principal axis of largest moment of inertia to align with the angular momentum, whereas  $\boldsymbol{\mu}$  will tend to be perpendicular to the principal axis of largest moment of inertia.

<sup>5</sup> The 10 $\mu\text{m}$  silicate feature does not appear in the emission spectrum of diffuse interstellar clouds (Onaka, et al. 1996), implying that the particles small enough to be heated to  $T_d \gtrsim 150\text{K}$  by single-photon heating do not have a significant silicate component.

<sup>6</sup> The IR drag torque depends on  $Qa^2 \propto a^3$ . The factor  $(a/a_x)^4$  enters in (30) and (31) from the normalization (14).

For small grains, the quantized heating by starlight photons results in thermal “spikes” followed by intervals of cooling (see, e.g., Draine & Anderson 1985), thereby altering the emission spectrum and affecting the rotational damping, as noted by Rouan et al (1992). As shown in Appendix C.2, if individual heating events may be treated separately, for very small carbonaceous grains we obtain (cf. eq. C26)

$$F_{\text{IR},q} = 4.49 a_{-7}^{1/2} \left( \frac{u_*}{u_{\text{ISRF}}} \right) \left( \frac{20 \text{ cm}^{-3}}{n_{\text{H}}} \right) T_2^{-1/2} \left( \frac{a}{a_x} \right)^4 . \quad (31)$$

We have  $F_{\text{IR},q} = F_{\text{IR},c}$  for  $a = a_{\text{IR}}$ , where

$$a_{\text{IR}} = 5.68 \times 10^{-7} \left( \frac{u_*}{u_{\text{ISRF}}} \right)^{-2/9} \text{ cm} . \quad (32)$$

We use eq.(30) for  $a > a_{\text{IR}}$ , and eq.(31) for  $a < a_{\text{IR}}$ , or

$$F_{\text{IR}} = \min(F_{\text{IR},q}, F_{\text{IR},c}) . \quad (33)$$

In Figs. 4 – 7 we show  $F_{\text{IR}}$  as a function of grain radius  $a$ .

#### 4.4. Electric Dipole Damping

The spinning grain will radiate power as given by eq. (12). The associated rotational damping time depends on  $\omega$ . It will prove convenient (see §6) to define a characteristic damping time

$$\tau_{ed} \equiv \frac{3I^2 c^3}{4\mu^2 kT} = \frac{16\pi^2 \xi^2 \rho^2 a^{10} c^3}{75 \mu^2 kT} \quad (34)$$

$$= 7.13 \times 10^{10} \text{ s} \frac{\xi^2 a_{-7}^8}{((a_x/a)^2 \langle Z^2 \rangle + 3.8(\beta/0.4\text{D})^2 a_{-7}) T_2} , \quad (35)$$

where we have assumed the dipole moment to be given by eq. (11). With  $\tau_{ed}$  defined by eq.(35), we see that electric dipole damping contributes

$$\left( \frac{1}{\omega} \frac{d\omega}{dt} \right)_{ed} = - \frac{I\omega^2}{3kT} \frac{1}{\tau_{ed}} . \quad (36)$$

In Figures 4 – 7 we show  $\tau_H/\tau_{ed}$  as a function of  $a$ .

#### 4.5. Relative Importance of Damping Mechanisms

Although all the processes discussed above contribute to rotational damping, some of them are more important than others. In *diffuse molecular clouds* (see Fig. 4) the plasma drag is dominant. This result is counterintuitive as the degree of ionization is small ( $x = 10^{-4}$ ). To understand this, recall that  $F_p \propto a^{-5}T^{-2}$ , so that for small grains and low temperatures plasma drag can dominate the gaseous drag, even when the fractional ionization is low. Dipole emission drag is of only marginal importance because of the relatively high gas density in the molecular region.

In *cold neutral media* (see Fig. 5) plasma drag  $F_p$  dominates in the range  $6 \times 10^{-8} \text{ cm} \lesssim a \lesssim 1.5 \times 10^{-7} \text{ cm}$ . For smaller grains damping via dipole emission is more important, while for larger grains infrared emission damping dominates. The infrared damping  $F_{IR} \propto a^{-1}$  for large grains (with steady temperatures) and  $F_{IR} \propto a^{1/2}$  for small ones (which undergo temperature “spikes”).

In *warm neutral media* (see Fig. 6) and in *warm ionized media* (see Fig. 7) the dipole emission is dominant for grains  $\lesssim 1.5 \times 10^{-7} \text{ cm}$  mostly as the consequence of less efficient coupling between grains and the surrounding gas. For larger grains infrared damping dominates. The difference between the two media evidently stems from the fractional ionization: in ionized media interactions with ions and plasma effects are more important than collisions with neutrals.

### 5. Rotational Excitation

#### 5.1. Recoil from Thermal Collisions and Evaporation

An initially stationary grain will have its rotational kinetic energy increasing at an average rate

$$\frac{d}{dt} \left( \frac{1}{2} I \omega^2 \right) = n_{\text{H}} \left( \frac{8kT}{\pi m_{\text{H}}} \right)^{1/2} \frac{2\pi a_x^4 m_{\text{H}} kT}{I} (G_n + G_i + G_p + G_{\text{IR}}) \quad , \quad (37)$$

where the normalized excitation rate  $G_n$  is due to impacting neutrals,  $G_i$  is due to impacting ions,  $G_p$  is due to plasma drag, and  $G_{\text{IR}}$  is due to recoil from infrared emission.

Neutrals deposit angular momentum when they impact the grain, and give the grain an additional kick when they subsequently evaporate. These processes (see Appendix B.2)

result in a normalized excitation rate

$$G_n = \sum_{Z_g} f(Z_g) \sum_n \frac{n_n}{2n_H} \left(\frac{m_n}{m_H}\right)^{1/2} \left\{ \exp(-Z_g^2 \epsilon_n^2) + 2Z_g^2 \epsilon_n^2 + \frac{T_{ev}}{T} [\exp(-Z_g^2 \epsilon_n^2 T/T_{ev}) + 2Z_g^2 \epsilon_n^2 T/T_{ev}] \right\} . \quad (38)$$

We separate the ion contribution into that delivered by incoming ions, and that due to the evaporating neutrals resulting from the ion collisions:

$$G_i = G_i^{(in)} + G_i^{(ev)} , \quad (39)$$

$$G_i^{(in)} = \sum_{Z_g \neq 0} f(Z_g) \sum_i \frac{n_i}{2n_H} \left(\frac{m_i}{m_H}\right)^{1/2} g_2(Z_i Z_g e^2 / a_s kT) + f(0) \sum_i \frac{n_i}{2n_H} \left(\frac{m_i}{m_H}\right)^{1/2} \left[ 1 + \frac{3\pi^{1/2}}{4} \phi + \frac{1}{2} \phi^2 \right] , \quad (40)$$

$$G_i^{(ev)} = \sum_{Z_g \neq 0} f(Z_g) \sum_i \frac{n_i}{2n_H} \left(\frac{m_i}{m_H}\right)^{1/2} g_1(Z_i Z_g e^2 / a_s kT) \frac{T_{ev}}{T} \times \left[ \frac{\exp(-Z_g^2 \epsilon_i^2) + 2Z_g^2 \epsilon_i^2}{\exp(-Z_g^2 \epsilon_i^2) + |Z_g| \epsilon_i \pi^{1/2} \text{erf}(|Z_g| \epsilon_i)} \right] + f(0) \sum_i \frac{n_i}{2n_H} \left(\frac{m_i}{m_H}\right)^{1/2} \frac{T_{ev}}{T} \left[ 1 + \frac{\pi^{1/2}}{2} \phi \right] , \quad (41)$$

$$g_2(x) = \begin{cases} 1 - x + x^2/2 & \text{if } x < 0 \\ e^{-x} & \text{if } x > 0 \end{cases} , \quad (42)$$

where we once again sum over neutrals  $n$  and ions  $i$ .  $\phi$  is defined by eq.(24) and  $\epsilon_i$  is defined by eq.(23) but using the polarizability of the species resulting from neutralization of the incoming ion  $i$ . In Figs. 8-11 we show  $G_n$  and  $G_i$  as functions of grain radius  $a$ . Coulomb attraction makes  $G_i$  the dominant excitation process for small grain.

## 5.2. Excitation by the Plasma

Excitation of grain rotation by the fluctuating electric field from passing ions is [cf. eq.(25)]

$$G_p = \frac{2e^2 \mu^2}{3a_x^4 (kT)^2} \sum_i \frac{n_i Z_i^2}{n_H} \left(\frac{m_i}{m_H}\right)^{1/2} \left\{ \ln(b_\omega/a) + \cos^2 \Psi \ln[\min(b_q, \lambda_D)/b_\omega] \right\} . \quad (43)$$

### 5.3. Infrared Emission

Each infrared photon carries away angular momentum  $\hbar$ , and hence there must be a corresponding change in the angular momentum of the grain. The energy in the radiated photons is due to absorption of starlight photons, but since there are  $\sim 500$  infrared photons emitted per starlight photon, we may neglect the angular momentum change due to the photon absorption event itself.

If the grain temperature is approximated as constant and we assume graphitic grains, then (see Appendix C.1)<sup>7</sup>

$$G_{\text{IR},c} = \frac{7.34}{a_{-7}} \left(\frac{a}{a_x}\right)^4 \left(\frac{u_*}{u_{\text{ISRF}}}\right)^{5/6} \left(\frac{20 \text{ cm}^{-3}}{n_{\text{H}}}\right) T_2^{-3/2} . \quad (44)$$

For very small grains, the grain temperature may be treated as zero except immediately following a photon absorption event, in which case for graphitic grains we find:

$$G_{\text{IR},q} = \frac{2.11}{a_{-7}^{1/4}} \left(\frac{a}{a_x}\right)^4 \left(\frac{u_*}{u_{\text{ISRF}}}\right) \left(\frac{20 \text{ cm}^{-3}}{n_{\text{H}}}\right) T_2^{-3/2} . \quad (45)$$

We take

$$G_{\text{IR}} = \min(G_{\text{IR},c}, G_{\text{IR},q}) . \quad (46)$$

### 5.4. Photoelectric Emission

The contribution to rotational excitation by photoelectrons emitted randomly from the grain is

$$G_{pe} = \frac{m_e}{4n_{\text{H}}(8\pi m_{\text{H}}kT)^{1/2}a_x^2kT} \sum_{Z_g} f(Z_g)\dot{N}_{pe} \left( \langle E_{pe} \rangle + \frac{(Z_g + 1)e^2}{a_s} \right) , \quad (47)$$

where  $\dot{N}_{pe}(Z_g)$  is the rate of emission of escaping photoelectrons from a grain with charge  $Z_g e$ , and  $\langle E_{pe} \rangle$  is the mean kinetic energy of the escaping photoelectrons at infinity. We assume the photoelectrons emerge from the grain surface with a “cosine-law” directional distribution.  $\langle E_{pe} \rangle$  is as estimated by Bakes & Tielens (1994). Because  $m_e \ll m_{\text{H}}$ , the contribution of photoelectric emission to rotational drag is negligible.

---

<sup>7</sup> The factor  $(a/a_x)^4$  in eq.(44) and (45) enters from the normalization of  $G$  [see eq.(37)].

### 5.5. Random H<sub>2</sub> Formation

If a fraction  $\gamma$  of arriving H atoms recombine at random on the grain surface, and the nascent H<sub>2</sub> has an average translational kinetic energy  $E_f$ , then the contribution to rotational excitation is

$$G_{\text{H}_2} = \frac{\gamma}{4}(1 - y) \frac{E_f}{kT} \left( 1 + \frac{\langle J(J+1) \rangle \hbar^2}{2m_{\text{H}} E_f a_x^2} \right) . \quad (48)$$

The nascent H<sub>2</sub> is assumed to leave the grain surface with a “cosine-law” directional distribution, with the internal angular momentum  $J\hbar$  uncorrelated with the velocity.

The efficiency  $\gamma$  of H<sub>2</sub> formation on very small grains is very uncertain, as is the effective number  $N_r$  of active recombination sites. For very small grains, H<sub>2</sub> formation may be suppressed due to temperature fluctuations (which limit the residence time of H atoms) or chemical “poisoning” (Lazarian 1995) of recombination sites, but the details are very uncertain. The empirical rate coefficient for H<sub>2</sub> formation on grains  $R \approx 3 \times 10^{-17} n(\text{H}) n_{\text{H}} \text{ cm}^3 \text{ s}^{-1}$  (Jura 1975) provides a limit: if small grains contribute a geometric cross section per H  $\sim 2 \times 10^{-21} \text{ cm}^2/\text{H}$  (see §9), then  $\gamma \lesssim 0.2$  if H<sub>2</sub> formation on small grains is not to exceed the empirically-determined total H<sub>2</sub> formation rate in the CNM.

In Figs. 8-11 we show  $G_{\text{H}_2}$  for  $\gamma = 0.1$ ,  $E_f = 0.2 \text{ eV}$ , and  $\langle J(J+1) \rangle = 10^2$ . We see that  $G_{\text{H}_2}$  does not make a major contribution to rotational excitation.

### 5.6. Systematic Torques

Suprathermal rotation may result if systematic torques act on a grain. Purcell first showed that various processes, including variations of the accommodation coefficient, photo-electric yield, and formation of hydrogen on preferential sites, can drive suprathermal rotation. Recently, radiative torques were identified as an important means of suprathermal spin-up (Draine & Weingartner 1996).

Thus far, suprathermal rotation has been discussed mostly in relation to grain alignment and for relatively large grains, i.e. with  $a > 10^{-6} \text{ cm}$  (see Lazarian & Draine 1997). The degree of suprathermality, i.e. the ratio of grain kinetic energy to its energy of thermal rotation, depends on grain size.

Systematic torques differ from the random torques in having a nonzero time average (in grain coordinates). Let  $\Gamma_s$  be a time-averaged systematic torque in grain coordinates. If the grain were not subject to fluctuating torques, it would attain a steady rotational

velocity  $\omega_s$  satisfying

$$\Gamma_s = \frac{IF\omega_s}{\tau_H} + \frac{4\mu^2\omega_s^3}{9c^3} . \quad (49)$$

For our purposes it is sufficient to use the simple approximation

$$\omega_s = \frac{\Gamma_s\tau_H}{IF} \left[ 1 + \frac{4\mu^2}{9\Gamma_s c^3} \left( \frac{\Gamma_s\tau_H}{IF} \right)^3 \right]^{-1/3} , \quad (50)$$

which is exact in the limits  $\Gamma \rightarrow 0$  and  $\Gamma_s \rightarrow \infty$ . The rate at which the systematic torque does work on the grain is then just  $\Gamma_s\omega_s$ .

The actual grain rotational velocity  $\omega$  is also the result of fluctuating torques, but  $\Gamma_s\omega_s$  remains a good estimate for the mean rate at which the systematic torque contributes to the rotational kinetic energy. Thus it is natural to characterize the importance of superthermal torques through a dimensionless quantity  $G_s$  defined by analogy with the dimensionless excitation rates  $G_n$ ,  $G_i$ , and  $G_p$ :

$$G_s \equiv \frac{I\Gamma_s\omega_s}{n_H(2\pi m_H kT)^{1/2} 4a_x^4 kT} , \quad (51)$$

where  $\omega_s$  is given by eq. (50).

Formation of  $H_2$  molecules on catalytic sites can drive superthermal rotation. Averaged over grains of radius  $a$ , the rms torque is<sup>8</sup>

$$\Gamma_s = \frac{4\gamma n(H)a_x^2 a_s}{N_r^{1/2}} (\pi m_H E_f kT)^{1/2} , \quad (52)$$

where  $\gamma$  is the fraction of impinging H atoms which leave the grain surface as  $H_2$ ,  $E_f = 0.2\hat{E}_f$  eV is the translational kinetic energy per nascent  $H_2$ ,  $N_r$  is the number of recombination sites on the grain surface, and we have assumed that at each recombination site the newly-formed  $H_2$  leaves the surface in a fixed direction, with the direction for each site randomly-drawn from a “cosine-law” distribution. Then, using eq.(50,51)

$$G_s \approx 1.75 \times 10^4 \frac{a_{-7}^3}{N_r} \left( \frac{a_s}{a} \right)^2 \left( \frac{a}{a_x} \right)^4 \frac{\xi \hat{E}_f \gamma^2}{FT_2} (1-y)^2 \left[ 1 + \frac{4\mu^2}{9\Gamma_s c^3} \left( \frac{\Gamma_s\tau_H}{IF} \right)^3 \right]^{-1/3} . \quad (53)$$

For large grains, we expect  $N_r \propto a^2$ , but for all grains where  $H_2$  forms ( $\gamma > 0$ ) we must have  $N_r \geq 1$ . We will consider two extreme cases:

---

<sup>8</sup> The rms moment-arm  $\propto (a_x^4/a_s^2)^{1/2}$ , and the  $H_2$  formation rate per site  $\propto a_s^2/N_r$ , hence  $\Gamma_s \propto a_x^2 a_s$ .



1. No H<sub>2</sub> formation:  $\gamma = 0$ ,  $\Gamma_s = 0$ , and  $G_s = 0$ .
2. H<sub>2</sub> formation with  $\gamma = 0.1$ ,  $\hat{E}_f = 1$ , and the number of recombination sites on a grain taken to be

$$N_r = 1 + \left( \frac{a}{2 \times 10^{-7} \text{ cm}} \right)^2 . \quad (54)$$

### 5.7. Relative Importance of Excitation Mechanisms

Unlike the case of the damping mechanisms, ion bombardment dominates rotational excitation for small grains in all ISM phases discussed above. This apparent disparity between damping and excitation processes, which seemingly contradicts the Fluctuation-Dissipation theorem, is the consequence of the non-equilibrium state of the interstellar medium. The ionization in  $T \lesssim 10^4\text{K}$  regions is primarily due to photoionization and cosmic rays, and far exceeds the ionization which would correspond to thermodynamic equilibrium at the kinetic temperature of the gas. The dominance of ion excitations stems from the increase of both capture cross section and angular momentum per capture.

In *molecular clouds* (see Fig. 8) excitation through ion collisions is dominant for grains  $\lesssim 1.7 \times 10^{-7}$  cm. As a result, these grains rotate with velocities a bit *larger* than would result from Brownian motion.

In *cold neutral media* the picture is more involved (see Fig. 9). Regular torques associated with H<sub>2</sub> formation can affect grain dynamics for  $a \gtrsim 10^{-7}$  cm. The rate of excitation through infrared emission is very close to that of gaseous bombardment in the range  $4 \times 10^{-8} \text{ cm} < a < 4 \times 10^{-7} \text{ cm}$  and only for larger grains do grain-neutral interactions dominate grain excitation.

The relative importance of ion excitations drops with grain temperature. Therefore for *warm neutral media* (see Fig. 10) collisions with ions constitute the leading excitation mechanism only for grains less than  $\sim 10^{-6}$  cm. For larger grains collisions with neutrals dominate. However, for *warm ionized media* (see Fig. 11), where 99% of species are ionized, collisions with ions are bound to be the major source of rotational excitation.

## 6. Rate of Rotation

With  $F$  defined by equation (14), the time-averaged rate of change of rotational kinetic energy may be written

$$0 = \left\langle \frac{d}{dt} \frac{I\omega^2}{2} \right\rangle = \frac{3kT}{\tau_H} G - I \frac{\langle \omega^2 \rangle}{\tau_H} F - \frac{4\mu^2}{9c^3} \langle \omega^4 \rangle \quad , \quad (55)$$

where

$$G \equiv G_n + G_i + G_p + G_{\text{IR}} + G_s \quad , \quad (56)$$

where  $G_s > 0$  if there are systematic torques due to  $\text{H}_2$  formation [eq.(53)]. Although the distribution of angular velocities will not be Maxwellian (except in the limit where electric dipole emission and superthermal torques are both negligible), we assume the relation between moments of a Maxwellian distribution,

$$\langle \omega^4 \rangle = \frac{5}{3} \langle \omega^2 \rangle^2 \quad , \quad (57)$$

to obtain a quadratic equation in  $\langle \omega^2 \rangle$  from eq. (55). With the electric dipole damping time  $\tau_{ed}$  defined by eq. (35), the solution is

$$\langle \omega^2 \rangle = \frac{2}{1 + [1 + (G/F^2)(20\tau_H/3\tau_{ed})]^{1/2}} \left( \frac{G}{F} \right) \left( \frac{3kT}{I} \right) \quad . \quad (58)$$

Eq. (58) provides a reasonable estimate for the rms grain rotation rate.

The effective rotational damping time  $\tau_J$  is given by

$$\frac{1}{\tau_J} = \frac{F}{\tau_H} + \left( \frac{I\omega^2}{3kT} \right) \frac{1}{\tau_{ed}} \quad . \quad (59)$$

## 7. Effects of Impulsive Torques

The above discussion of grain rotation has been directed at estimating  $\langle \omega^4 \rangle$  for grains of radius  $a$ . Because we do not have thermal equilibrium, however, the angular velocity distribution may depart substantially from a Maxwellian. In particular, if  $I\delta\omega$  is the angular momentum of an impacting particle, then if  $\langle \delta\omega^2 \rangle \gtrsim \langle \omega^2 \rangle$ , then the angular velocity distribution will depart from a Maxwellian. This occurs when infrared emission and/or electric dipole emission is able to reduce the grain angular velocity substantially between impact events.

One can show that colliding species  $j$  has

$$\langle(\delta\omega)^2\rangle_j = (G_j/F_j)2a^2m_jkT/I^2 \quad . \quad (60)$$

In Figure 13 we show  $\langle(\delta\omega)^2\rangle$  for impacting ions, normalized by  $\langle\omega^2\rangle$  for the grain. We see that for large grains, the impulsive nature of the rotational excitation is unimportant, and the time evolution of the grain rotation can be treated as a continuous process. For grains with  $a \lesssim 7 \text{ \AA}$ , however, a single ion impact can change the grain angular momentum substantially. From Fig. 9 we see that ion impacts are the dominant source of rotational excitation for small grains in the MC, CNM, and WIM phases. This is primarily the result of the strong electric dipole damping for small grains (see Figs. 5 – 7) in diffuse gas, which causes the smaller grains to have sub-thermal rates of rotation.

## 8. Centrifugal Stresses

An upper limit for the grain rotational frequency  $\omega$  can be obtained from the ability of grains to withstand centrifugal stress (Draine & Salpeter 1979). With a characteristic stress  $(1/4)\rho\omega^2a_x^2$ , and a maximum stress  $S_{max}$ , the maximum rotational frequency is

$$\frac{\omega}{2\pi} \lesssim \frac{1}{\pi a_x} \left( \frac{S_{max}}{\rho} \right)^{1/2} = 7 \times 10^{10} \frac{1}{a_{-7}} \left( \frac{a}{a_x} \right) \left( \frac{S_{max}}{10^9 \text{ ergs cm}^{-3}} \right)^{1/2} \text{ Hz} \quad . \quad (61)$$

Bulk polycrystalline substances have  $S_{max} \approx 10^9 \text{ ergs cm}^{-3}$ , while for single-crystal materials  $S_{max} \approx 10^{11} \text{ ergs cm}^{-3}$ . As can be seen from Figure 12, the expected rotation rates are such that even grains with  $S_{max}$  as small as  $10^9 \text{ ergs cm}^{-3}$  can survive.

## 9. Size Distribution

### 9.1. Diffuse Clouds

As shown below, microwave emission from grains is only significant for  $\omega/2\pi \gtrsim 1 \text{ GHz}$ , so from Fig. 12 we see that only  $a \lesssim 3 \times 10^{-7} \text{ cm}$  grains ( $N \lesssim 10^4$ ) are of capable of contributing to such emission.

The size distribution of these ultrasmall dust grains is very poorly known. Studies of interstellar extinction are relatively insensitive to the detailed distribution of very small dust grains. Observations of extinction at  $\lambda \gtrsim 1000 \text{ \AA}$  constrain the total mass in dust at  $a \lesssim 1 \times 10^{-6} \text{ cm}$ , but do not reveal how this mass is distributed over grains of different sizes.

The MRN distribution (Mathis, Rumpl, & Nordsieck 1977), extended down to very small sizes, provides one estimate for the population of very small grains. The graphitic component has

$$\frac{dn}{da} = n_{\text{H}} A_{\text{MRN}} a^{-3.5} \quad \text{for } a_{\text{min}} < a < 2.5 \times 10^{-5} \text{ cm}, \quad (62)$$

with  $A_{\text{MRN}} = 10^{-25.16} \text{ cm}^{2.5}$  (Draine & Lee 1984). This size distribution, if extended down to  $a_{\text{min}} = 3.6 \text{ \AA}$ , has 17% of the grain mass in  $a < 10^{-6} \text{ cm}$  grains, but only 2.6% of the mass is in  $a < 10^{-7} \text{ cm}$  grains. This distribution of graphitic grains would contribute a geometric cross section per H atom  $\Sigma_{\text{MRN}} = 2.2 \times 10^{-21} \text{ cm}^2$ .

Observations of the ‘‘UIR’’ emission features, as well as the strong  $12\mu\text{m}$  and  $25\mu\text{m}$  emission observed by IRAS (Boulanger & Péroult 1988), have been interpreted as showing that there must be a substantial population of very small grains (Leger & Puget 1984; Draine & Anderson 1985). Here we consider a log-normal size distribution for this population, which we add to the MRN distribution:

$$\frac{1}{n_{\text{H}}} \frac{dn}{da} = A_{\text{MRN}} a^{-3.5} + B a^{-1} \exp \left[ -\frac{1}{2} \left( \frac{\ln(a/a_0)}{\sigma} \right)^2 \right]. \quad (63)$$

We will consider  $a_0 = 6 \text{ \AA}$  and  $\sigma = 0.4$ ; The coefficient  $B$  is chosen so that the grains contain a fraction  $f_{\text{C}} = 0.05$  of the total carbon abundance ( $\text{C}/\text{H} = 4.0 \times 10^{-4}$ ; Grevesse et al. 1991). This grain component then contributes an additional geometric cross section per H atom  $\Sigma = 1.7 \times 10^{-21} \text{ cm}^2$ .

For comparison, we note that the grain model of Désert, Boulanger, and Puget (1990) has  $f_{\text{C}} = 0.09$  in the ‘‘PAH’’ component, molecules with  $60 < N < 540$  C atoms.

## 9.2. Dense Clouds

The abundance of ultrasmall grains in dense interstellar clouds is not well known. In denser regions, the wavelength  $\lambda_{\text{max}}$  of maximum polarization is increased, and the ratio  $R_V \equiv A_V/E(B - V) \approx 5.5$ , significantly larger than the value  $R_V \approx 3.1$  characteristic of diffuse regions; both are indications that the fraction of the grain mass in smaller grains is reduced in denser regions. Here we will assume that the fraction of the mass in ultrasmall grains is reduced by a factor 5 relative to diffuse clouds: for  $a \lesssim 3 \times 10^{-7} \text{ cm}$  we adopt the size distribution (63) but with  $A_{\text{MRN}}$  and  $B$  reduced by a factor 5 from the values used for diffuse clouds.

## 10. Emissivity

Recognizing that there will be a range of dipole moments among grains of a given size, we will assume that 25% of the grains have  $\beta = 0.5\beta_0$ , 50% have  $\beta = \beta_0$ , and 25% have  $\beta = 2\beta_0$ , with  $\beta_0 = 0.4$  debye as our standard value.

For each grain size  $a$  and value of  $\beta$ , there is a mean square angular velocity  $\langle\omega^2\rangle$ . If we assume  $\omega$  to follow a Boltzmann distribution, then the emissivity per H is

$$\frac{j_\nu}{n_H} = \left(\frac{8}{3\pi}\right)^{1/2} \frac{1}{n_H c^3} \int da \frac{dn}{da} \frac{\mu^2 \omega^6}{\langle\omega^2\rangle^{3/2}} \exp\left(\frac{-3\omega^2}{2\langle\omega^2\rangle}\right) . \quad (64)$$

We evaluate this emissivity for the size distribution of Fig. 14, for conditions characteristic of different phases of the interstellar medium. We consider the case where no H<sub>2</sub> formation takes place, as well as the case where it occurs with 10% efficiency ( $\gamma = 0.1$ ).

Ferrara & Dettmar (1994) predicted the microwave emission from grains under WIM conditions, obtaining an emissivity  $j_\nu/n_H = 1.1 \times 10^{-15}(\nu/100 \text{ GHz})^{2.8} \text{ Jy sr}^{-1}$ . The slope and magnitude of this emission is similar to our results near 10 GHz, but this is coincidental: Ferrara & Dettmar assumed grains to be rotating with thermal rotation rates corresponding to  $\sim 10^4\text{K}$ , whereas we find very strong damping by both microwave emission and infrared emission (see Fig. 7) so that the grains actually rotate very subthermally (relative to the 8000K gas temperature in the WIM). For example, for  $a = 10^{-7}$  cm grains under WIM conditions, we estimate  $\omega_{rad}/2\pi \approx 8.5 \text{ GHz}$  (see Fig. 12), whereas Ferrara & Dettmar estimate a rotation rate  $\sim 50 \text{ GHz}$  for this size; since the emitted power  $\propto \omega^4$ , this is a significant difference. In Ferrara & Dettmar’s model, the 10 GHz emission comes from grains with  $a \approx 2 \times 10^{-7}$  cm, whereas we find here that the 10 GHz emission comes primarily from grains with  $a \approx 9 \times 10^{-8}$  cm; these two sizes differ by a factor of  $\sim 10$  in mass, and  $\sim 50$  in moment of inertia.

In Figure 16 we show the effects of decreasing the intrinsic dipole moments  $\mu_i$  by a factor of two, by taking  $\beta_0 = 0.2$  debye and  $\epsilon = 0.05$ . In Figure 17 we show the emissivity calculated for H<sub>2</sub> formation efficiencies  $\gamma = 0$  and 0.1; the spectra are essentially unchanged. It is apparent that the emission spectra are not especially sensitive to the precise values of  $\beta_0$  or  $\gamma$ .

It is evident that the population of small grains which has been inferred previously from observations of both the UIR emission features and the 12 and 25 $\mu\text{m}$  *IRAS* emission should produce substantial electric dipole emission in the 10–100 GHz region.

It appears that this emission has already been detected by experiments designed to measure angular structure in the cosmic background radiation. Kogut et al. (1996), de

Oliveira-Costa et al (1997), and Leitch et al. (1997) have reported detection of 14 – 90 GHz microwave emission which is correlated with 100 $\mu$ m emission, and therefore apparently originates in interstellar gas or dust. Draine & Lazarian (1998) argue that this emission is in fact due to rotational emission from spinning dust grains in diffuse interstellar gas at high galactic latitudes. The observed emissivity per H nucleon is shown in Figs. 15 – 16, and it is seen that the observed emissivities are in fact approximately equal to the electric dipole emission predicted here. Future measurements of the spectrum of this diffuse emission, and its correlation with interstellar gas and dust, will test this interpretation, although the emission is weak because of the relatively small amounts of dust at high galactic latitudes. The *MAP* mission, to be launched in 2000, is expected to obtain accurate maps of the emission from interstellar dust in five bands, from 22 – 90 GHz.

## 11. Detecting Dark Clouds

It may also be possible to detect emission from spinning dust grains in dense clouds, where the larger column densities result in increased intensities. As an example, we consider the central surface brightness for the model which Lazarian, Goodman & Myers (1997) adopt for the L1755 dark cloud, with a central column density  $N_{\text{H}} = 2 \times 10^{22} \text{ cm}^{-2}$  in material with densities  $n_{\text{H}} \approx 10^4 \text{ cm}^{-3}$ , plus  $N_{\text{H}} = 1.3 \times 10^{21} \text{ cm}^{-2}$  in diffuse molecular gas with  $n_{\text{H}} \approx 300 \text{ cm}^{-3}$ . To this we add  $N_{\text{H}} = 1 \times 10^{21} \text{ cm}^{-2}$  in HI surrounding the cloud, with conditions characteristic of the CNM phase.

We add vibrational (“thermal”) emission to the rotational emission, using dust temperatures of 12K, 15K, and 18K for dark regions, diffuse molecular gas, and CNM, respectively; the assumed dust opacity is  $\propto \nu^{1.7}$  and reproduces the observed  $\lambda \gtrsim 100\mu\text{m}$  emission from the interstellar medium for a grain temperature  $T_d \approx 18\text{K}$ . Figure 18 shows the resulting spectrum. We see that at 10 – 30 GHz antenna temperatures of  $\sim 1\text{mK}$  are expected toward the central regions; for the adopted cloud model about half of this emission originates in the extended “CNM” envelope of the cloud.

## 12. Discussion

We have presented above a detailed study of rotational excitation and damping for grains with sizes less than  $\sim 10^{-6} \text{ cm}$ . In addition to processes included in earlier work by Rouan et al. (1992), we have included both direct collisions with ions and “plasma drag”. Ion collisions and plasma drag, together with damping by infrared and microwave

emission, dominate rotational excitation and damping for most interstellar environments. It is therefore important to include these processes in other studies of rotational excitation, such as those proposing to explain features of the diffuse interstellar bands (Rouan, Leger, & Coupanec 1997).

For the assumed distribution of grain sizes and electric dipole moments, we predict microwave emission from spinning dust grains which can account for the “anomalous emission” observed recently in the 15–90 GHz range. The predicted intensities are uncertain, however, as they depend on three poorly-known factors:

1. The abundances and size distribution of the small grains. This uncertainty is greatest in the case of dense/dark regions, where the absence of starlight denies us the evidence (12 – 25 $\mu$ m emission) which requires an abundance of ultrasmall grains in diffuse regions.
2. The charge distribution of the small grains, which affects the rates of rotational excitation and damping. We have used standard estimates for photoelectric cross sections (Bakes & Tielens 1994) and electron capture cross sections (Draine & Sutin 1987) for very small grains. The uncertainties in these quantities affect both the electric dipole moment and, more importantly, the rate of angular momentum exchange with ions.
3. The electric dipole moments of both neutral and charged small grains.

The shape of the small grains (chainlike vs. sheetlike vs. quasispherical) is also uncertain, but is less critical than the above factors. A fifth factor – the efficiency of H<sub>2</sub> formation on small grains – is not critical for these estimates: in Fig. 12 only the grains in the CNM show appreciable sensitivity to whether or not H<sub>2</sub> formation takes place, and even for the CNM component the emissivity at  $\nu \gtrsim 2$  GHz is only slightly changed (see Fig. 17).

Because of these uncertainties, definitive predictions for the rotational emission spectrum are not yet possible. Nevertheless, within the existing theoretical and observational uncertainties it appears that much or all of the observed 15–90 GHz “anomalous” emission is due to spinning dust grains. The largest discrepancy between observation and theory is at 14.5 GHz, where Leitch et al. report emission about 3.5 times stronger than the emission predicted in Fig. 15. Additional measurements at  $\nu \lesssim 20$  GHz will be of great value to clarify whether this emission has another origin, or whether some of our assumptions concerning the dust must be modified.

Emission from rotating grains must be allowed for in studies of the cosmic microwave background radiation (see DL98). It appears that the small rotating grains may be partially

aligned with the local magnetic field (Lazarian & Draine 1998), so that the electric dipole radiation will be linearly polarized; this may present a problem for interpretation of CMB polarization measurements by the MAP mission.

### 13. Summary

The principal results of this paper are as follows:

1. Even neutral dust grains are expected to usually have electric dipole moments arising from polarized chemical bonds within the grain. Charged grains have an additional contribution to the dipole moment due to displacement of the charge centroid from the mass centroid. Our estimate for the dipole moment is given by eq. (11).
2. The excitation and damping of rotation in small grains is determined by collisions with ions and neutrals, “plasma drag”, emission of infrared and microwave radiation, and formation of H<sub>2</sub> on the grain surface. Ion collisions and plasma drag, omitted in previous estimates of rotation rates, are included in the present analysis and found to often dominate rotational excitation and damping. Induced-dipole attraction of neutrals by charged grains, and of ions by neutral grains, can also be significant. Because the charge state of the grain, and the fractional ionization of the gas, do not reflect thermodynamic equilibrium, the fluctuation-dissipation theorem does not directly apply.
3. For very small grains ( $a \lesssim 7 \times 10^{-8}$  cm), the angular momentum of colliding ions is large compared to the r.m.s. angular momentum of the grain, and therefore the grain rotation history consists of “rotational spikes” separated by intervals of gradual rotational damping.
4. The estimated grain rotation rates are such that the small grains which have been postulated to explain the near-infrared emission feature can account for the emission observed at 30 – 50 GHz by Kogut et al., de Oliveira-Costa et al., and Leitch et al. (1997).
5. The emission observed at 14.5 GHz by Leitch et al. is stronger than we estimate for spinning grains by a factor  $\sim 4$ . Additional determinations of emission from dust at frequencies  $\lesssim 20$  GHz will be of great value.
6. We predict that dark clouds should produce detectable microwave emission, with antenna temperatures of  $\gtrsim 1$ mK at  $\sim 10 - 30$  GHz.



We are grateful to David Spergel for attracting our attention to this problem, and to Robert Lupton for the availability of the SM package. We thank W.D. Watson for helpful comments. B.T.D. acknowledges the support of NSF grant AST-9619429, and A.L. the support of NASA grant NAG5-2858.

### A. Geometric Factors

For cylindrical grains ( $a < a_1$ ) of diameter  $d$  and length  $2b$  we have

$$b = \frac{8a^3}{3d^2} \quad , \quad (\text{A1})$$

$$a_s = \left[ \frac{bd}{2} + \frac{d^2}{8} \right]^{1/2} \quad , \quad (\text{A2})$$

$$a_x = \left[ \frac{b^3d}{6} + \frac{b^2d^2}{8} + \frac{bd^3}{8} + \frac{d^4}{64} \right]^{1/4} \quad , \quad (\text{A3})$$

$$\xi = \frac{160}{27} \left( \frac{a}{d} \right)^4 \quad . \quad (\text{A4})$$

where the “surface-equivalent” radius  $a_s$  and “excitation-equivalent” radius  $a_x$  are defined in eq.(2,3), and  $\xi \equiv I/(0.4Ma^2)$ . For disklike grains ( $a_1 < a < a_2$ ) of thickness  $d$  and radius  $b$  we have

$$b = \left( \frac{4a^3}{3d} \right)^{1/2} \quad , \quad (\text{A5})$$

$$a_s = \left[ \frac{b^2}{2} + \frac{bd}{2} \right]^{1/2} \quad , \quad (\text{A6})$$

$$a_x = \left[ \frac{b^4}{4} + \frac{b^3d}{2} + \frac{b^2d^2}{8} + \frac{bd^3}{24} \right]^{1/4} \quad , \quad (\text{A7})$$

$$\xi = \frac{5a}{3d} \quad . \quad (\text{A8})$$

For spheres ( $a > a_2$ ),  $a_s = a_x = a$  and  $\xi = 1$ . Figure 19 shows how  $a_s/a$ ,  $a_x/a$  and  $\xi$  vary with  $a$ .

### B. Rotational Damping and Excitation of Grains in a Partially Ionized Gas

The angular momentum of a spherical grain in a partially-ionized gas changes due to several distinct scattering processes:

1. impact of neutral atoms and molecules on the grain surface;
2. impact of ions on the grain surface;

3. electromagnetic interaction of the electric dipole moment of the grain with passing ions.

Each of these processes contributes to both rotational excitation and rotational damping.

The microphysics of inelastic scattering of particles which impact directly on the grain surface is obviously complex. We idealize the problem by imagining that species which arrive at a point on the grain surface are re-emitted from the same point on the grain surface with a thermal distribution of velocities in the frame of reference of the local (moving) grain surface at the instant of emission. Thus we neglect possible effects of large centripetal accelerations of the grain surface when the grain is rotating rapidly. We further assume that all arriving neutrals and ions depart the grain surface as neutrals.

With this idealization, we can now calculate the rate of rotational damping and rotational excitation. The drag and rotational excitation from different components is additive.

### B.1. General Considerations

Consider a spherical grain of radius  $a$  and moment of inertia  $I = (8\pi/15)\rho a^5$ , with charge  $Z_g e$ , rotating with angular velocity  $\omega$ . Atoms and molecules arrive at the surface with (on average) zero net angular momentum. Angular momentum is carried away by the gas atoms and molecules which are re-emitted from the surface, so the rate of damping is directly proportional to the rate at which mass arrives at the grain surface. In order to more easily compare different contributions, we will “normalize” to the rate of damping which would be contributed by only the H atoms in neutral atomic gas:

$$\frac{-1}{\omega} \frac{d}{dt} I \omega = \left[ n_{\text{H}} \left( \frac{8kT}{\pi m_{\text{H}}} \right)^{1/2} \pi a^2 m_{\text{H}} \frac{2a^2}{3} \right] F \quad , \quad (\text{B1})$$

with  $F = 1$  for neutral grains and H atoms in atomic gas. The drag processes are additive, so that

$$F = \sum_j F_j \quad , \quad (\text{B2})$$

where  $F_j$  is the contribution to  $F$  from process  $j$ .

Suppose that the interaction potential is such that particles of species  $x$  with velocity  $v$  at infinity collide with the grain surface if and only if the impact parameter  $b \leq b_{\text{max}}(v)$ .

Then collisions with species  $x$  contribute

$$F_x = \frac{n_x}{n_H} \left( \frac{m_x}{m_H} \right)^{1/2} \left( \frac{\pi m_x}{8kT} \right)^{1/2} \int_0^\infty dv \, 4\pi v^2 f_x(v) v \left( \frac{b_{max}(v)}{a} \right)^2, \quad (\text{B3})$$

where

$$f_x(v) \equiv \left( \frac{m_x}{2\pi kT} \right)^{3/2} \exp(-m_x v^2/kT) \quad . \quad (\text{B4})$$

We also consider the rate at which collisions act to increase  $J^2$  for a stationary grain, and again normalize to the rate which would be appropriate for H atoms in neutral atomic gas if the atoms left the grain as H atoms at temperature  $T$ :

$$\left\langle \frac{d}{dt} J^2 \right\rangle_{\omega=0} = \left[ n_H \left( \frac{8kT}{\pi m_H} \right)^{1/2} 4\pi a^4 m_H kT \right] G \quad . \quad (\text{B5})$$

For a given grain, we will consider the contributions  $G_j$  which various processes  $j$  make to the overall excitation rate  $G$ . The incoming particles contribute

$$G_x^{(in)} = \frac{n_x}{n_H} \left( \frac{m_x}{m_H} \right)^{1/2} \frac{\pi^{1/2}}{8} \left( \frac{m_x}{2kT} \right)^{3/2} \int_0^\infty dv \, 4\pi v^2 f_x(v) v^3 \left( \frac{b_{max}(v)}{a} \right)^4 \quad . \quad (\text{B6})$$

Each arriving particle, after delivering its incoming angular momentum to the grain, later “evaporates” and escapes from the grain surface. We assume that evaporating particles have a velocity distribution appropriate for a grain temperature  $T_{ev}$ . Because the evaporating particles interact with the grain (some evaporating particles will not have “escape velocity” and will return to the grain surface), we use the fact that the angular momentum distribution of escaping particles must equal that for the same species being captured from a gas at temperature  $T_{ev}$ . Thus one can show that the evaporating particles contribute

$$G_x^{(ev)} = \frac{m_x}{8a^2 kT} \Delta F \left\{ \frac{\int_0^\infty dv f_x^{(ev)}(v) v^5 [b_{max}^{(ev)}(v)]^4}{\int_0^\infty dv f_x^{(ev)}(v) v^3 [b_{max}^{(ev)}(v)]^2} \right\}, \quad (\text{B7})$$

where  $f_x^{(ev)}(v)$  is given by eq.(B4) but with  $T$  replaced by  $T_{ev}$ , and  $b_{max}^{(ev)}(v)$  is the value of  $b_{max}$  appropriate for particles with the physical properties of the evaporating species (i.e., neutrals even when the impinging species  $x$  is an ion).

## B.2. Neutral-Grain Collisions

Prior to impact, the grain-neutral interaction is approximated by an induced dipole potential,

$$U(r) = -\frac{1}{2} \alpha_n \frac{Z_g^2 e^2}{r^4} \quad (\text{B8})$$

where  $\alpha_n$  is the polarizability of the neutral atom or molecule, and  $Z_g e$  is the charge on the grain. The trajectories of particles in an  $r^{-4}$  potential are well-known (see, e.g., Wannier 1953, Osterbrock 1961). For an atom with initial velocity  $v$ , impact parameters

$$b < b_0(v) \equiv \left( \frac{4Z_g^2 e^2 \alpha_n}{mv^2} \right)^{1/4} \quad (\text{B9})$$

have “spiral” trajectories which pass through the origin, while for  $b > b_0$  trajectories are “hyperbolic”, with a finite distance of closest approach. A hyperbolic trajectory with  $b = b_0$  has a distance of closest approach  $r_{min} = b_0/\sqrt{2}$ . Thus we may use the condition  $a = b_0/\sqrt{2}$  to define a velocity

$$v_a \equiv \left( \frac{Z_g^2 e^2 \alpha_n}{ma^4} \right)^{1/2} \quad (\text{B10})$$

such that

$$b_{max}(v) = \begin{cases} b_0(v) & \text{if } v \leq v_a \\ a \left( 1 + \frac{Z_g^2 e^2 \alpha_n}{ma^4 v^2} \right)^{1/2} & \text{if } v \geq v_a \end{cases} \quad (\text{B11})$$

Thus the contribution to  $F$  is

$$F_n = \frac{n_n}{n_H} \left( \frac{m_n}{m_H} \right)^{1/2} \left[ \exp(-\epsilon_n^2) + \epsilon_n \pi^{1/2} \text{erf}(\epsilon_n) \right] \quad (\text{B12})$$

where

$$\epsilon_n^2 \equiv \frac{mv_a^2}{2kT} = \frac{Z_g^2 e^2 \alpha_n}{2a^4 kT} \quad (\text{B13})$$

The contribution of neutral species  $n$  to  $G$  is

$$G_n = \left( \frac{T + T_{ev}}{2T} \right) \frac{n_n}{n_H} \left( \frac{m_n}{m_H} \right)^{1/2} \left[ \exp(-\epsilon_n^2) + 2\epsilon_n^2 \right] \quad (\text{B14})$$

### B.3. Ion-Grain Collisions

#### B.3.1. Charged Grain: $Z_g \neq 0$

For a Coulomb law potential  $Z_g Z_i e^2 / r$ , we have (Spitzer 1941)

$$b_{max}(v) = \begin{cases} 0 & \text{for } \frac{mv^2}{2} < \frac{Z_g Z_i e^2}{a} \\ a \left( 1 - \frac{2Z_g Z_i e^2}{mav^2} \right)^{1/2} & \text{for } \frac{mv^2}{2} > \frac{Z_g Z_i e^2}{a} \end{cases} \quad (\text{B15})$$

For ions and charged grains ( $Z_g Z_i \neq 0$ ) we neglect the modifications to  $b_{max}$  which result when the “image charge” contribution to the interaction is taken into consideration (see

Draine & Sutin 1987, and §B.3.2 below). The contribution of colliding ions to  $F$  is then (Spitzer 1941)

$$F_i = \frac{n_i}{n_H} \left( \frac{m_i}{m_H} \right)^{1/2} g_1(\psi) \quad \text{for } Z_i Z_g \neq 0 \quad , \quad (\text{B16})$$

$$\psi \equiv \frac{Z_g Z_i e^2}{akT} \quad , \quad (\text{B17})$$

$$g_1(x) = \begin{cases} 1 - x & \text{if } x < 0 \\ e^{-x} & \text{if } x > 0 \end{cases} \quad . \quad (\text{B18})$$

The contribution to  $G$  due to the arriving ions is (Anderson & Watson 1993)

$$G_i^{(in)} = \frac{1}{2} \frac{n_i}{n_H} \left( \frac{m_i}{m_H} \right)^{1/2} g_2(\psi) \quad , \quad (\text{B19})$$

$$g_2(x) = \begin{cases} 1 - x + x^2/2 & \text{if } x < 0 \\ e^{-x} & \text{if } x > 0 \end{cases} \quad . \quad (\text{B20})$$

We assume the ions to depart from the grain as neutrals. Per departing neutral, we should have the same contribution to  $G$  as for arriving neutrals if the gas temperature were  $T_{ev}$  (see eq. B12 and B14). Thus departing neutrals contribute

$$G_i^{(ev)} = F_i \frac{T_{ev}}{2T} \left[ \frac{\exp(-Z_g^2 \epsilon_i^2) + 2Z_g^2 \epsilon_i^2}{\exp(-Z_g^2 \epsilon_i^2) + |Z_g| \epsilon_i \pi^{1/2} \text{erf}(|Z_g| \epsilon_i)} \right] \quad , \quad (\text{B21})$$

where

$$\epsilon_i^2 \equiv \frac{e^2 \alpha_i}{2a^4 k T_{ev}} \quad , \quad (\text{B22})$$

where  $\alpha_i$  is the polarizability of the neutral obtained from ion  $i$ .

### B.3.2. Neutral Grain: $Z_g = 0$

In the case of a neutral grain, the collision rate is modified by the polarization of the grain by the electric field of the ion. If the grain is approximated as a perfect conductor, the interaction potential is

$$U(r) = -\frac{Z_i^2 e^2 a^3}{2r^2(r^2 - a^2)} \quad . \quad (\text{B23})$$

The collision rate for this interaction potential has been discussed by Draine & Sutin (1987). Using their eq. (B6),<sup>9</sup> with  $\nu = 0$ , gives a critical impact parameter

$$b_{max}(v) = a \left[ 1 + \left( \frac{4Z_i^2 e^2}{mv_0^2 a} \right)^{1/2} \right]^{1/2}, \quad (\text{B24})$$

so that

$$F_i = \frac{n_i}{n_H} \left( \frac{m_i}{m_H} \right)^{1/2} \left[ 1 + \frac{\pi^{1/2}}{2} \phi \right]. \quad (\text{B25})$$

The arriving ions contribute

$$G_i^{(in)} = \frac{1}{2} \frac{n_i}{n_H} \left( \frac{m_i}{m_H} \right)^{1/2} \left[ 1 + \frac{3\pi^{1/2}}{4} \phi + \frac{1}{2} \phi^2 \right], \quad (\text{B26})$$

where

$$\phi^2 \equiv \frac{2Z_i^2 e^2}{akT}, \quad (\text{B27})$$

and the departing neutrals contribute an additional

$$G_i^{(ev)} = \frac{T_{ev}}{2T} \Delta F. \quad (\text{B28})$$

#### B.4. Plasma Drag

Consider a stationary grain with electric dipole moment  $\boldsymbol{\mu}$ . The electric field  $\mathbf{E}$  at the grain due to nearby ions exerts a torque  $\boldsymbol{\mu} \times \mathbf{E}$ . To estimate the effects of such torques, we assume that an ion with impact parameter  $b$  passes on a straight-line trajectory at constant velocity  $\mathbf{v}$ . To define the orientation of  $\boldsymbol{\mu}$ , let the direction of  $\mathbf{v}$  define a polar axis, with  $\theta$  the angle between  $\mathbf{v}$  and  $\boldsymbol{\mu}$ , and let the azimuthal angle  $\phi = 0$  when  $\boldsymbol{\mu}$  is in the plane containing both the ion trajectory and the grain. It is then easy to show that the angular momentum  $\Delta J$  exchanged between the ion and the grain has

$$(\Delta J)^2 = \left( \frac{2\mu Z_i e}{bv} \right)^2 (\sin^2 \theta \sin^2 \phi + \cos^2 \theta). \quad (\text{B29})$$

If we now average over random orientation of  $\boldsymbol{\mu}$  ( $\langle \sin^2 \theta \rangle = 2/3$ ,  $\langle \cos^2 \theta \rangle = 1/3$ ,  $\langle \sin^2 \phi \rangle = 1/2$ ) and then over a thermal distribution of velocities  $v$ , we find (Anderson &

---

<sup>9</sup> Note the typographical error in eq. (B6) of Draine & Sutin (1987), which should read  $(2\epsilon x - \nu)(x^2 - 1)^2 - x = 0$ .

Watson 1993)

$$\begin{aligned} \frac{d}{dt}J^2 &= n_i \int_0^\infty dv 4\pi v^2 f_i(v) v \int_{b_1}^{b_2} 2\pi b db \frac{2}{3} \left( \frac{2\mu Z_i e}{bv} \right)^2 \\ &= \frac{8\pi}{3} n_i \left( \frac{8kT}{\pi m_i} \right)^{1/2} \frac{Z_i^2 e^2 m_i}{kT} \mu^2 \ln(b_2/b_1) \quad . \end{aligned} \quad (\text{B30})$$

For the lower cutoff we simply take the grain radius  $b_1 = a$ . The upper cutoff is more problematic. It is clear that it cannot exceed the Debye length,

$$b_2 \leq \lambda_D \equiv \left( \frac{kT}{4\pi n_e e^2} \right)^{1/2} = 398 \left( \frac{T/100\text{K}}{n_e/0.03 \text{ cm}^{-3}} \right)^{1/2} \text{ cm} \quad , \quad (\text{B31})$$

since at larger distances the ion electric field is screened. However, for a grain rotating at angular velocity  $\omega > 0$ , an ion with velocity  $v_{th} = (2kT/m_i)^{1/2}$  and impact parameter  $b \gtrsim b_\omega \equiv v_{th}$  will be almost unaffected by the rotating component of the grain dipole moment, as the torque averaged over the grain rotation will tend to zero. For a grain with a thermal rotation rate  $\omega \approx (2kT/I)^{1/2}$  we have

$$b_\omega \approx \left( \frac{8\pi\xi\rho a^5}{15m_i} \right)^{1/2} = 4.5 \times 10^{-6} a_{-7}^{2.5} \xi^{1/2} \left( \frac{m_H}{m_i} \right)^{1/2} \text{ cm} \quad . \quad (\text{B32})$$

Let  $\Psi$  be the angle between the dipole moment  $\boldsymbol{\mu}$  and the rotation velocity  $\boldsymbol{\omega}$ . In eq.(B31) we would then replace

$$\mu^2 \ln(b_2/b_1) \rightarrow \mu^2 \left[ \ln(b_\omega/b_1) + \cos^2 \Psi \ln(b_2/b_\omega) \right] \quad (\text{B33})$$

We differ here from the treatment of Anderson & Watson (1993) who neglected the contribution of impact parameters  $b > b_\omega$ . The rotational excitation is quantized, and we expect the above classical estimate to fail when the characteristic frequency  $\sim v_{th}/b$  of the time-varying electric field from the passing ion varies falls below the frequency  $\hbar/I$  of the  $J = 0 \rightarrow 1$  rotational transition, resulting in a ‘‘quantum’’ cutoff  $b_q \approx I v_{th}/\hbar$ , or

$$b_q = 4.1 \times 10^{-3} \xi a_{-7}^5 \left( \frac{T/100\text{K}}{m_i/m_H} \right)^{1/2} \text{ cm} \quad . \quad (\text{B34})$$

Passing ions then contribute<sup>10</sup>

$$\frac{dJ^2}{dt} = \frac{16}{3} n_i \left( \frac{2\pi m_i}{kT} \right)^{1/2} Z_i^2 e^2 \mu^2 \left\{ \ln(b_\omega/a_s) + \cos^2 \Psi \ln [\min(b_q, \lambda_D)/b_\omega] \right\} \quad , \quad (\text{B35})$$

---

<sup>10</sup> It is instructive to compare B35 with quantum-mechanical calculations. For CN ( $\mu = 1.45$  debye) and  $T = 10^4\text{K}$  the rate coefficient for  $J/\hbar = 0 \rightarrow 1$  excitation by protons is  $\langle \sigma v \rangle_{0 \rightarrow 1} \approx 4 \times 10^{-6} \text{ cm}^3 \text{ s}^{-1}$  (Thaddeus 1972), whereas taking  $\cos^2 \Psi = 1$  we estimate  $(2n_i \hbar^2)^{-1} dJ^2/dt \approx 1.5 \times 10^{-5} \text{ cm}^3 \text{ s}^{-1}$ , too large by a factor  $\sim 4$ . Such agreement even for a case where quantum effects are dominant is reassuring.



$$G_p = \frac{n_i}{n_H} \left( \frac{m_i}{m_H} \right)^{1/2} \frac{2Z_i^2 e^2}{3a_x^4 (kT)^2} \mu^2 \left\{ \ln(b_\omega/a_s) + \cos^2 \Psi \ln [\min(b_q, \lambda_D)/b_\omega] \right\} . \quad (\text{B36})$$

Having estimated the excitation rate  $G_p$ , we may now invoke the fluctuation-dissipation theorem to see that the normalized contribution to the damping rate must be simply  $F_p = G_p$ , so that if torques from passing ions were the only torques present, the grain would attain a thermal rotational distribution.

## C. Damping and Excitation of Rotation by IR Emission

### C.1. Steady Emission

Suppose that the grain at rest contains six rotating electric dipoles, each with electric dipole moment  $p$  and with angular velocity  $\omega$  in grain body coordinates. There is one dipole rotating clockwise and one counterclockwise around each of the  $x$ –,  $y$ –, and  $z$ –axes. The dipoles emit incoherently, so that at rest the power radiated is just

$$\frac{dE}{dt} = 6 \times \frac{2\omega^4 p^2}{3c^3} ; \quad (\text{C1})$$

the emission is isotropic and unpolarized. Each dipole emits radiation which, in directions parallel to the dipole’s rotation axis, is 100% circularly polarized. For an individual dipole the angular momentum loss  $dL^{(1)}/dt$  is just

$$\frac{dJ^{(1)}}{dt} = \frac{2\omega^3 p^2}{3c^3} . \quad (\text{C2})$$

A system of two oppositely rotating dipoles radiates a net angular momentum if the whole system rotates with frequency  $\omega_r$  along the dipoles’ rotation axis: in the rest frame the frequencies of emission for the two dipoles are, respectively,  $\omega + \omega_r$  and  $\omega - \omega_r$ .

Let the system of six dipoles rotate around the  $x$ -axis with frequency  $\omega_r \ll \omega$ . The rate of loss of angular momentum associated with the single emission frequency  $\omega \gg \omega_r$  is then

$$\frac{dJ}{dt} = \left[ \frac{2(\omega + \omega_r)^3}{3c^3} - \frac{2(\omega - \omega_r)^3}{3c^3} \right] p^2 \approx \frac{\omega_r}{\omega^2} \frac{dE}{dt} . \quad (\text{C3})$$

Using the Planck expression for thermal emissivity we find

$$\frac{dJ}{dt} = -\omega_r a^2 \int_0^\infty \frac{Q_\nu B_\nu}{\nu^2} d\nu , \quad (\text{C4})$$

while

$$\frac{dE}{dt} = -4\pi^2 a^2 \int_0^\infty Q_\nu B_\nu d\nu \quad . \quad (\text{C5})$$

Now suppose

$$Q_\nu = Q_0 \left( \frac{\nu}{\nu_0} \right)^\beta \quad , \quad (\text{C6})$$

where we will assume  $\beta = 2$  for interstellar dust (Draine & Lee 1984), and set

$$\frac{dE}{dt} = -\pi a^2 \langle Q \rangle_* u_* c \quad , \quad (\text{C7})$$

where  $u_*$  is the energy density of starlight, and  $\langle Q \rangle_*$  is the grain absorption efficiency averaged over the starlight spectrum. Then

$$\frac{dJ}{dt} = -\frac{h^2 \Gamma(\beta + 2) \zeta(\beta + 2) \langle Q \rangle_* a^2 u_* c}{4\pi \Gamma(\beta + 4) \zeta(\beta + 4) (kT_d)^2} \quad , \quad (\text{C8})$$

where  $\Gamma$  and  $\zeta$  are the usual gamma function and Riemann  $\zeta$ -function. Thus

$$F_{\text{IR},c} = \frac{3}{(8\pi)^{3/2}} \frac{\Gamma(\beta + 2) \zeta(\beta + 2)}{\Gamma(\beta + 4) \zeta(\beta + 4)} \frac{\langle Q \rangle_* u_* c h^2}{n_{\text{H}} (m_{\text{H}} kT)^{1/2} (akT_d)^2} \quad (\text{C9})$$

$$= \frac{59.0}{a_{-7}} \left( \frac{u_*}{u_{\text{ISRF}}} \right) \left( \frac{20 \text{ cm}^{-3}}{n_{\text{H}}} \right) \left( \frac{100\text{K}}{T} \right)^{1/2} \left( \frac{20\text{K}}{T_d} \right)^2 \quad . \quad (\text{C10})$$

The grain temperature  $T_d$  and starlight intensity  $u_*$  are related through

$$T_d = \frac{hc}{k} \left[ \frac{\langle Q \rangle_* u_*}{8\pi hc Q_0 \lambda_0^\beta \Gamma(\beta + 4) \zeta(\beta + 4)} \right]^{1/(\beta+4)} \quad (\text{C11})$$

where  $\lambda_0 = c/\nu_0$ . We consider three grain materials: graphite, “astronomical silicate”, and  $\alpha$ -SiC (Draine & Lee 1984; Laor & Draine 1993), for each of which the infrared emissivity has  $\beta = 2$ , so that  $T_d \propto u_*^{1/6}$ .

The recoil from photon emission is a source of rotational excitation. For a nonrotating grain with radius  $a \ll hc/kT_d$ ,

$$\frac{d}{dt} J^2 = \frac{dN_{\text{ph}}}{dt} \hbar^2 \quad , \quad (\text{C12})$$

where the photon emission rate is

$$\frac{dN_{\text{ph}}}{dt} = \frac{\Gamma(\beta + 3) \zeta(\beta + 3)}{\Gamma(\beta + 4) \zeta(\beta + 4)} \frac{1}{kT_d} \pi a^2 \langle Q \rangle_* u_* c \quad . \quad (\text{C13})$$

Thus

$$G_{\text{IR},c} = \frac{\langle Q \rangle_* u_* h^2 c}{16 n_{\text{H}} m_{\text{H}}^{1/2} (2\pi kT)^{3/2} a^2 kT_d} \frac{\Gamma(\beta + 3) \zeta(\beta + 3)}{\Gamma(\beta + 4) \zeta(\beta + 4)} \quad . \quad (\text{C14})$$

## C.2. Thermal Spikes

Grains undergo a sudden temperature rise following each photon absorption. For very small grains, the temperature history can be regarded as a sequence of independent “thermal spikes”, separated by intervals where the grain is very cold. Rouan et al. (1992) discussed the rotational damping for a vibrational density of states chosen to approximate a PAH molecule. Here we adopt the Debye model for the heat capacity of the  $3N - 6$  vibrational modes (Kittel 1972). If  $\Theta$  is the Debye temperature, the thermal energy content for  $T \ll \Theta$  is

$$E = \frac{3\pi^4}{5}(N - 2)kT \left(\frac{T}{\Theta}\right)^3 . \quad (\text{C15})$$

The absorbed energy of a UV photon first heats the grain and then is emitted in the infrared. From (C5) and (C8) we obtain

$$\frac{dJ}{dE} = \frac{\omega_r}{4\pi^2} \frac{h^2}{(kT)^2} \frac{\Gamma(\beta + 2)\zeta(\beta + 2)}{\Gamma(\beta + 4)\zeta(\beta + 4)} . \quad (\text{C16})$$

Using (C15) to eliminate  $T$  in favor of  $E$ , we integrate to obtain the angular momentum loss in cooling from initial energy  $E$  to  $T = 0$ :

$$\delta J = -A\omega_r E^{1/2} , \quad (\text{C17})$$

$$A \equiv \frac{h^2}{2} \left(\frac{3}{5}\right)^{1/2} \frac{\Gamma(\beta + 2)\zeta(\beta + 2)}{\Gamma(\beta + 4)\zeta(\beta + 4)} \frac{(N - 2)^{1/2}}{(k\Theta)^{3/2}} . \quad (\text{C18})$$

The energy  $E$  is provided by the interstellar radiation field. Therefore

$$\frac{dJ}{dt} = -A\omega_r \int_0^\infty d\nu \left(\frac{cu_\nu}{h\nu}\right) Q_\nu (h\nu)^{1/2} \pi a^2 . \quad (\text{C19})$$

Define

$$\mathcal{F} \equiv \int_0^\infty d\nu \frac{cu_\nu}{h\nu} , \quad (\text{C20})$$

$$\langle E \rangle_{\mathcal{F}} \equiv \frac{1}{\mathcal{F}} \int d\nu cu_\nu , \quad (\text{C21})$$

$$\langle Q \rangle_{\mathcal{F}} \equiv \frac{1}{\mathcal{F}} \int_0^\infty d\nu \left(\frac{cu_\nu}{h\nu}\right) Q_\nu , \quad (\text{C22})$$

$$\langle Q \rangle_{\mathcal{F}E} \equiv \frac{1}{\mathcal{F}} \int_0^\infty d\nu cu_\nu Q_\nu , \quad (\text{C23})$$

$$\langle E^\gamma \rangle_{\mathcal{F}Q} \equiv \frac{1}{\mathcal{F}\langle Q \rangle_{\mathcal{F}}} \int_0^\infty d\nu \left(\frac{cu_\nu}{h\nu}\right) Q_\nu (h\nu)^\gamma . \quad (\text{C24})$$

Then

$$\frac{dJ}{dt} = -A\omega_r \mathcal{F}\langle Q \rangle_{\mathcal{F}} \langle E^{1/2} \rangle_{\mathcal{F}Q} \pi a^2 \quad . \quad (\text{C25})$$

Thus

$$F_{\text{IR},q} = \frac{3}{8} \left( \frac{3\pi}{10} \right)^{1/2} \frac{\Gamma(\beta + 2)\zeta(\beta + 2)}{\Gamma(\beta + 4)\zeta(\beta + 4)} \frac{h^2(N - 2)^{1/2}}{a^2(k\Theta)^{3/2}} \frac{\mathcal{F}\langle Q \rangle_{\mathcal{F}} \langle E^{1/2} \rangle_{\mathcal{F}Q}}{n_{\text{H}}(m_{\text{H}}kT)^{1/2}} \quad . \quad (\text{C26})$$

Because  $\langle Q \rangle_{\mathcal{F}} \propto a$ ,  $F_{\text{IR},q} \propto (N - 2)^{1/2}/a$ .

The emission following each heating event also contributes to the rotational excitation of the grain, with

$$\Delta J^2 = \frac{h^2 \Gamma(\beta + 3)\zeta(\beta + 3)}{3\pi \Gamma(\beta + 4)\zeta(\beta + 4)} (N - 2)^{1/4} \left( \frac{E}{k\Theta} \right)^{3/4} \quad . \quad (\text{C27})$$

Thus

$$G_{\text{IR},q} = \left[ \frac{h^2 \Gamma(\beta + 3)\zeta(\beta + 3)}{3\pi \Gamma(\beta + 4)\zeta(\beta + 4)} \frac{(N - 2)^{1/4}}{(k\Theta)^{3/4}} \right] \frac{\mathcal{F}\langle Q \rangle_{\mathcal{F}} \langle E^{3/4} \rangle_{\mathcal{F}Q}}{n_{\text{H}}(8kTm_{\text{H}}/\pi)^{1/2} 4a^2kT} \quad . \quad (\text{C28})$$

$\langle Q \rangle_{\mathcal{F}}$ ,  $\langle E^{1/2} \rangle_{\mathcal{F}Q}$ , and  $\langle E^{3/4} \rangle_{\mathcal{F}Q}$  were calculated for small graphite and silicate spheres for the interstellar radiation spectrum of Mezger, Mathis, & Panagia (1982) and Mathis, Mezger, & Panagia (1983). The results are presented in Table 4

Table 1: Idealized phases for interstellar matter.

phase	DC	MC	CNM	WNM	WIM
$n_{\text{H}}(\text{cm}^{-3})$	$10^4$	300.	30	0.4	0.1
$T(\text{K})$	10.	20.	100.	6000.	8000.
$\chi$	$10^{-4}$	0.01	1.	1.	1.
$x_{\text{H}} \equiv n(\text{H}^+)/n_{\text{H}}$	0	0	0.0012	0.1	0.99
$x_{\text{M}} \equiv n(\text{M}^+)/n_{\text{H}}$	$10^{-6}$	0.0001	0.0003	0.0003	0.001
$y \equiv 2n(\text{H}_2)/n_{\text{H}}$	0.999	0.99	0.	0.	0.

Table 2: Electric Dipole Moments for Selected Bonds<sup>a</sup>

bond	$\mu$
aliphatic C–H	0.3
aliphatic C=O	2.4
aromatic C=O	2.65
aromatic C–OH	1.6
aliphatic C–OH	1.7
aromatic C–CH <sub>3</sub>	0.37
aromatic C–C≡CH	0.7
aliphatic C–C≡CH	0.9
aromatic C–CHO	2.96
aliphatic C–CHO	2.49

<sup>a</sup> Dean (1992)

Table 3: Electric Dipole Moments for Selected Molecules

molecule	$N$	$\mu$	$\beta$
$C_5H_8$ 1 pentyne (trans) <sup>a</sup>	13	0.84	0.23
$C_7H_5N$ benzonitrile <sup>a</sup>	13	4.18	1.16
$HC_{11}N$ cyanopolyynes <sup>b</sup>	13	5.47	1.52
$C_5H_{10}O$ cyclopentanol <sup>a</sup>	16	1.72	0.43
$C_8H_{10}$ ethylbenzene <sup>a</sup>	18	0.59	0.14
$C_8H_{10}$ orthoxylene <sup>a</sup>	18	0.62	0.15
$C_{12}H_{10}$ acenaphthene <sup>a</sup>	22	0.85	0.18

<sup>a</sup> CRC Handbook (1997)

<sup>b</sup> Bell et al. (1997)

Table 4: Dust Grain Properties for Interstellar Starlight

quantity	graphite	silicate	$\alpha$ -SiC
$\langle Q \rangle_{\mathcal{F}}/a_{-7}$	$3.12 \times 10^{-3}$	$5.79 \times 10^{-4}$	$9.06 \times 10^{-4}$
$\langle Q \rangle_{\mathcal{F}E}/a_{-7}$	$8.92 \times 10^{-3}$	$3.20 \times 10^{-3}$	$8.45 \times 10^{-3}$
$\langle E^{1/2} \rangle_{\mathcal{F}Q}^2$	2.56 eV	4.63 eV	9.41 eV
$\langle E^{3/4} \rangle_{\mathcal{F}Q}^{4/3}$	2.78 eV	5.28 eV	9.68 eV
$\langle E \rangle_{\mathcal{F}Q}$	3.03 eV	5.86 eV	9.87 eV
$Q(100\mu\text{m})/a_{-7}$	$1.93 \times 10^{-3}$	$1.44 \times 10^{-5}$	$9.03 \times 10^{-7}$
$T_d(\text{ISRF})$	19.7 K	17.4 K	32.5 K

Assuming interstellar starlight (Mathis, Mezger, & Panagia 1982; Mezger, Mathis & Panagia 1983) with  $\mathcal{F} = 1.525 \times 10^{10} \text{ cm}^{-2} \text{ s}^{-1}$ ,  $u_{\text{ISRF}} = 8.626 \times 10^{-13} \text{ ergs cm}^{-3}$ , and  $\langle E \rangle_{\mathcal{F}} = 1.058 \text{ eV}$ . See eq.(C20–C23).

## REFERENCES

- Anderson, N., & Watson, W.D. 1993, *A&A*, 270, 477
- Bakes, E.L.O., & Tielens, A.G.G.M. 1994, *ApJ*, 427, 822
- Bell, M.B., Feldman, P.A., Travers, M.J., McCarthy, M.C., Gottlieb, C.A., & Thaddeus, P. 1997, *ApJ*, 483, L61
- Boulanger, F., & Pérouault, M. 1988, *ApJ*, 330, 964
- CRC Handbook of Chemistry and Physics, ed. D.R. Lide (Boca Raton: CRC Press)
- Dean, J.A. 1992, *Lange's Handbook of Chemistry*, 14th ed. (New York: McGraw-Hill)
- Désert, F.X., Boulanger, F., & Puget, J.L. 1990
- de Oliveira-Costa, A., Kogut, A., Devlin, M.J., Netterfield, C.B., Page, L.A., & Wollack, E.J. 1997, *ApJ*, 482, L17
- Draine, B.T., & Anderson, N. 1985, *ApJ*, 292, 494
- Draine, B.T., & Lazarian, A. 1998, *ApJ*, 494, L19 (DL98)
- Draine, B.T., & Lee, H.M. 1984, *ApJ*, 285, 89
- Draine, B.T., & Salpeter, E.E. 1979, *ApJ*, 231, 77
- Draine, B.T., & Sutin, B. 1987, *ApJ*, 320, 803
- Draine, B.T., & Weingartner, J.C. 1996, *ApJ*, 470, 551.
- Ferrara, A., & Dettmar, R.-J. 1994, *ApJ*, 427, 155
- Grevesse, N., Lambert, D.L., Sauval, A.J., van Dishoeck, E.F., Farmer, C.B., & Norton, R.H. 1991, *A&A* 242, 488
- Jones, R.V., & Spitzer, L. 1967, *ApJ*, 147, 943
- Jura, M. 1975, *ApJ*, 197, 575
- Kittel, C. 1972, *Introduction to Solid State Physics*, (New York: Wiley)
- Laor, A., & Draine, B.T. 1993, *ApJ*, 402, 441
- Lazarian, A. 1995, *MNRAS*, 274, 679

- Lazarian, A., & Draine, B.T. 1997, ApJ, 487, 248
- Lazarian, A., & Draine, B.T. 1998, in preparation
- Lazarian, A., Goodman, A.A., & Myers, P.C. 1997, ApJ, 490, 273
- Leger, A., & Puget, J.L. 1984, ApJ, 278, L19
- Leitch, E.M., Readhead, A.C.S., Pearson, T.J., & Myers, S.T. 1997, ApJ, 486, L23.
- Martin, P.G. 1972, MNRAS, 158, 63
- Mathis, J.S., Mezger, P.G., & Panagia, N. 1983, A&A, 128, 212
- Mathis, J.S., Rumpl, W., & Nordsieck, K.H., ApJ, 217, 425
- Mezger, P.G., Mathis, J.S., & Panagia, N. 1982, A&A, 105, 372
- Omont, A. 1986, A&A, 164, 159
- Onaka, T., Yamamura, I., Tanabé, T., Roellig, T., & Yuen, L. 1996, PASJ, 48, L59
- Osterbrock, D.E. 1961, ApJ, 134, 270
- Purcell, E.M. 1976, ApJ, 206, 685
- Purcell, E.M. 1979, ApJ, 231, 404.
- Purcell, E.M., & Spitzer, L. 1971, ApJ, 167, 31
- Reynolds, R.J. 1991, ApJ, 373, L17
- Rouan, D., Léger, A., & Coupanec, P 1997, A&A, 324, 661
- Rouan, D., Léger, A., Omont, A, & Giard, M. 1992, A&A, 253, 498
- Spitzer, L. 1941, ApJ, 93, 369
- Thaddeus, P. 1972, ARA&A, 10, 305
- Thaddeus, P. 1995, in *The Diffuse Interstellar Bands*, eds. A.G.G.M. Tielens & T.P. Snow (Dordrecht: Kluwer), 369
- Wannier, G.H. 1953, Bell System Tech. J., 32, 170
- Weingartner, J.C., & Draine, B.T. 1998, in preparation



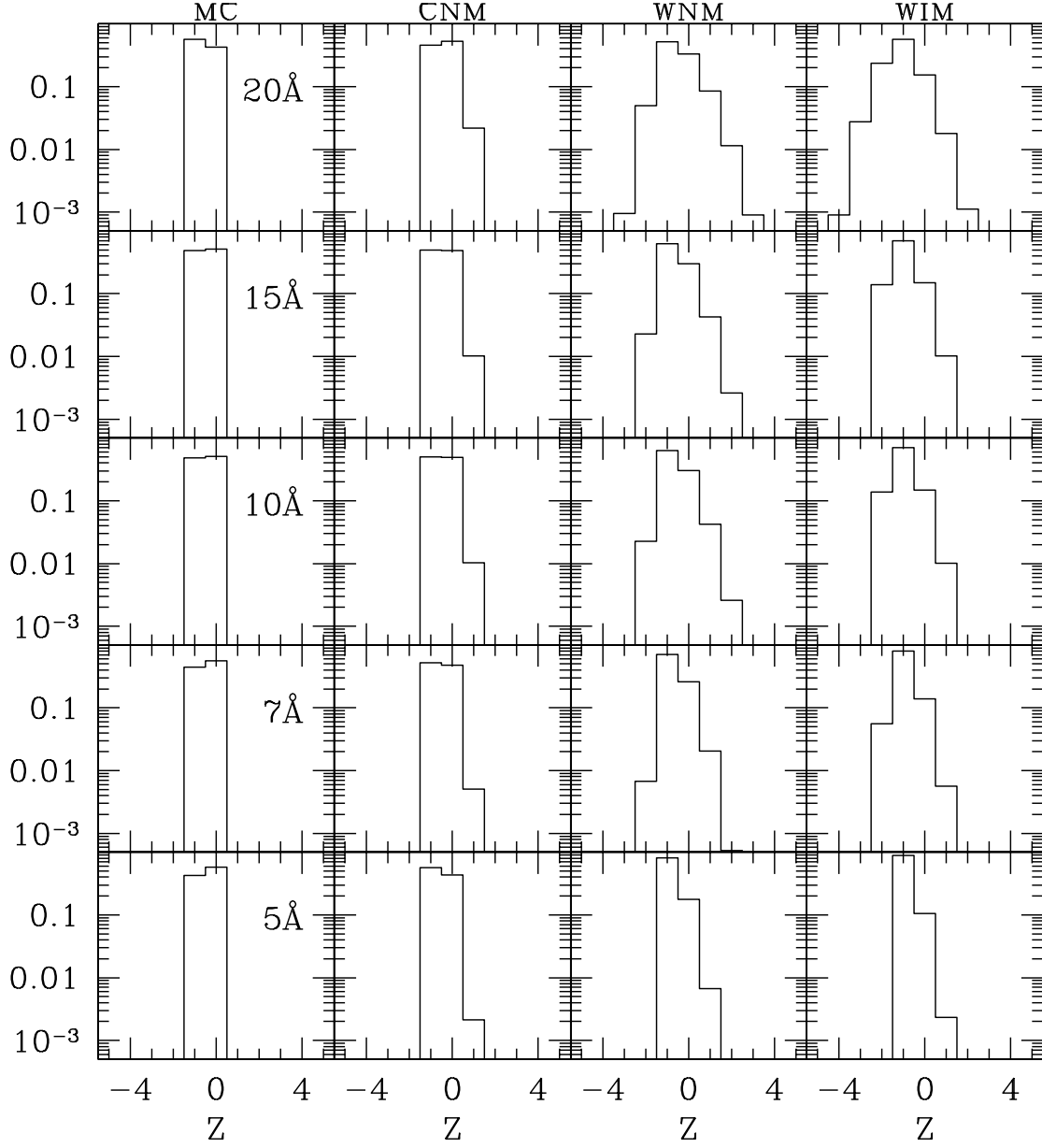


Fig. 1.— Charge distribution functions for grains of radii  $a = 5, 7, 10, 15, 20 \text{ \AA}$  for “Molecular Cloud” (MC), “Cold Neutral Medium” (CNM), “Warm Neutral Medium” (WNM), and “Warm Ionized Medium” (WIM) conditions.

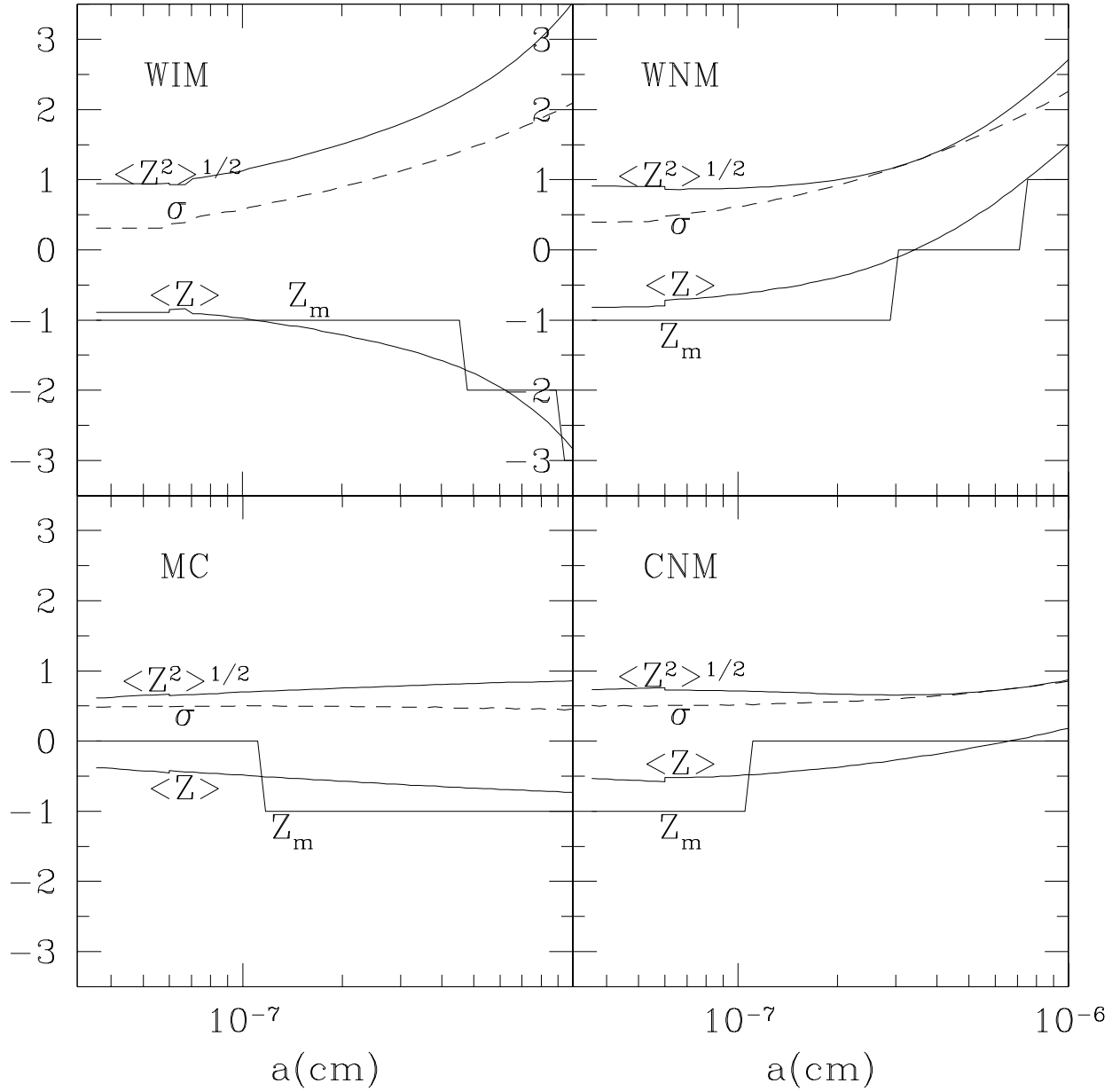


Fig. 2.— Mode  $Z_m$ , centroid  $\langle Z \rangle$ , rms charge  $\langle Z^2 \rangle^{1/2}$ , and standard deviation  $\sigma_Z$  for grains of radius  $a$  for CNM and WNM conditions.

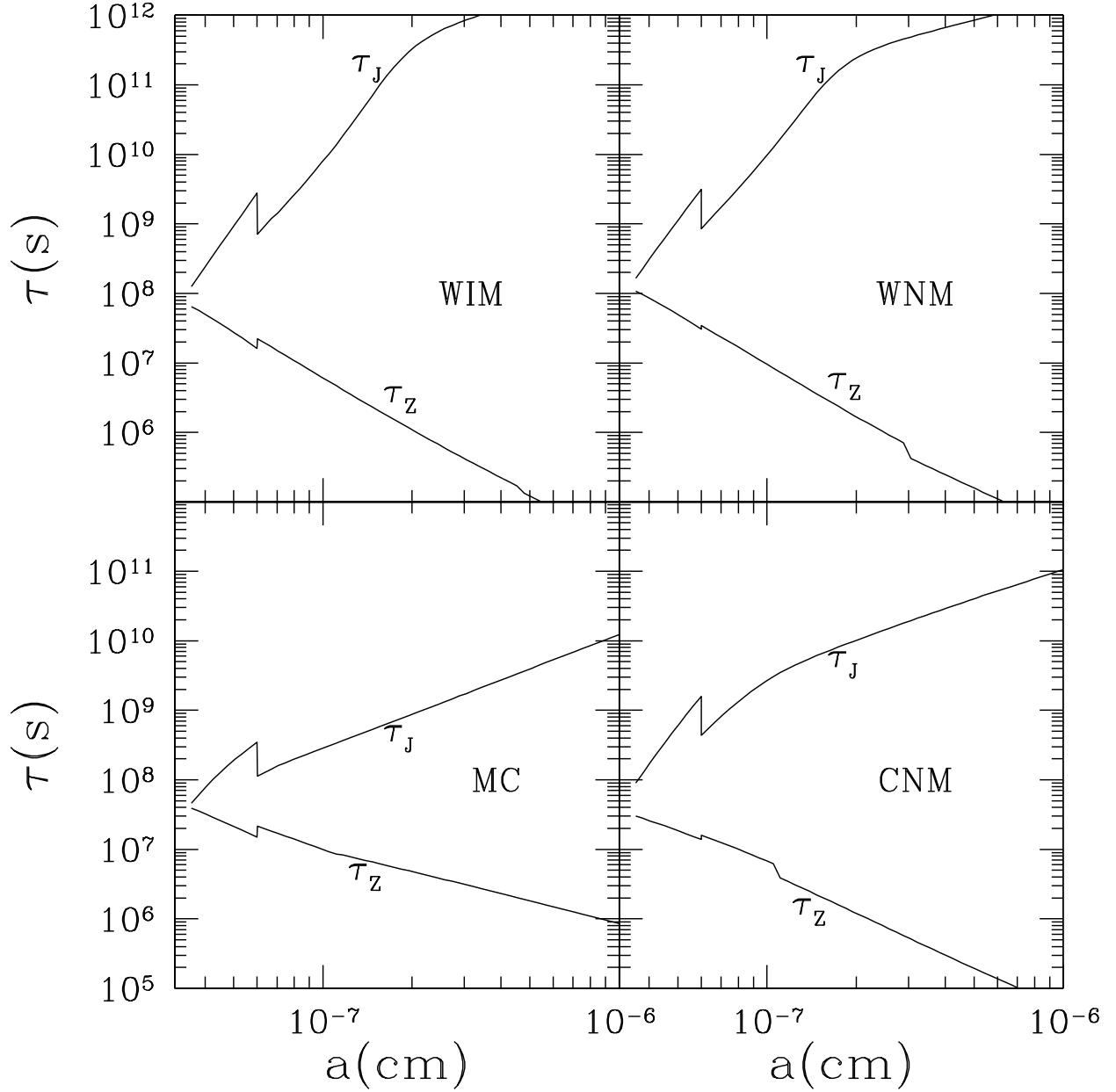


Fig. 3.— Characteristic time scale  $\tau_Z$  [see eq. (5)] for changes in the grain charge  $Ze$ . Also shown is the characteristic rotational damping time  $\tau_J$  [see eq. (59)] for a grain with charge  $Z_m e$ . It is apparent that the approximation  $\tau_Z \ll \tau_J$  is excellent for all except the smallest ( $a < 4 \text{ \AA}$ ) grains.

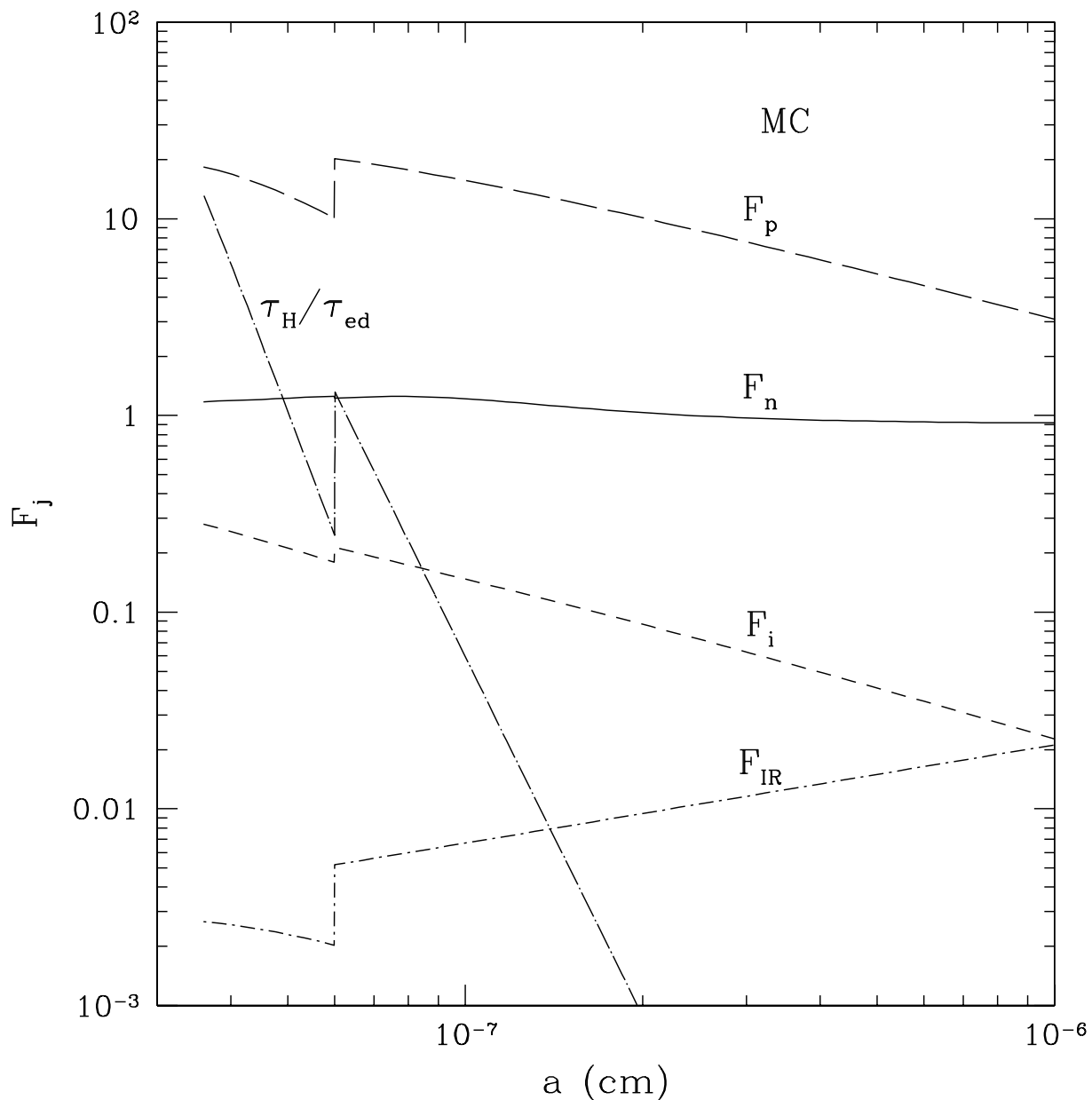


Fig. 4.— Dimensionless rotational drag functions for neutral collisions [ $F_n$ , eq.(19)], ion collisions [ $F_i$ , eq.(20)], plasma drag [ $F_p$ , eq.(25)], and infrared emission [ $F_{IR}$ , eq.(30-33)], for “Molecular Cloud” conditions. Plasma drag is more important than other gas collisional processes. Also shown is the ratio  $\tau_H/\tau_{ed}$  showing the relative importance of electric dipole damping. For molecular cloud conditions, electric dipole damping is not important.

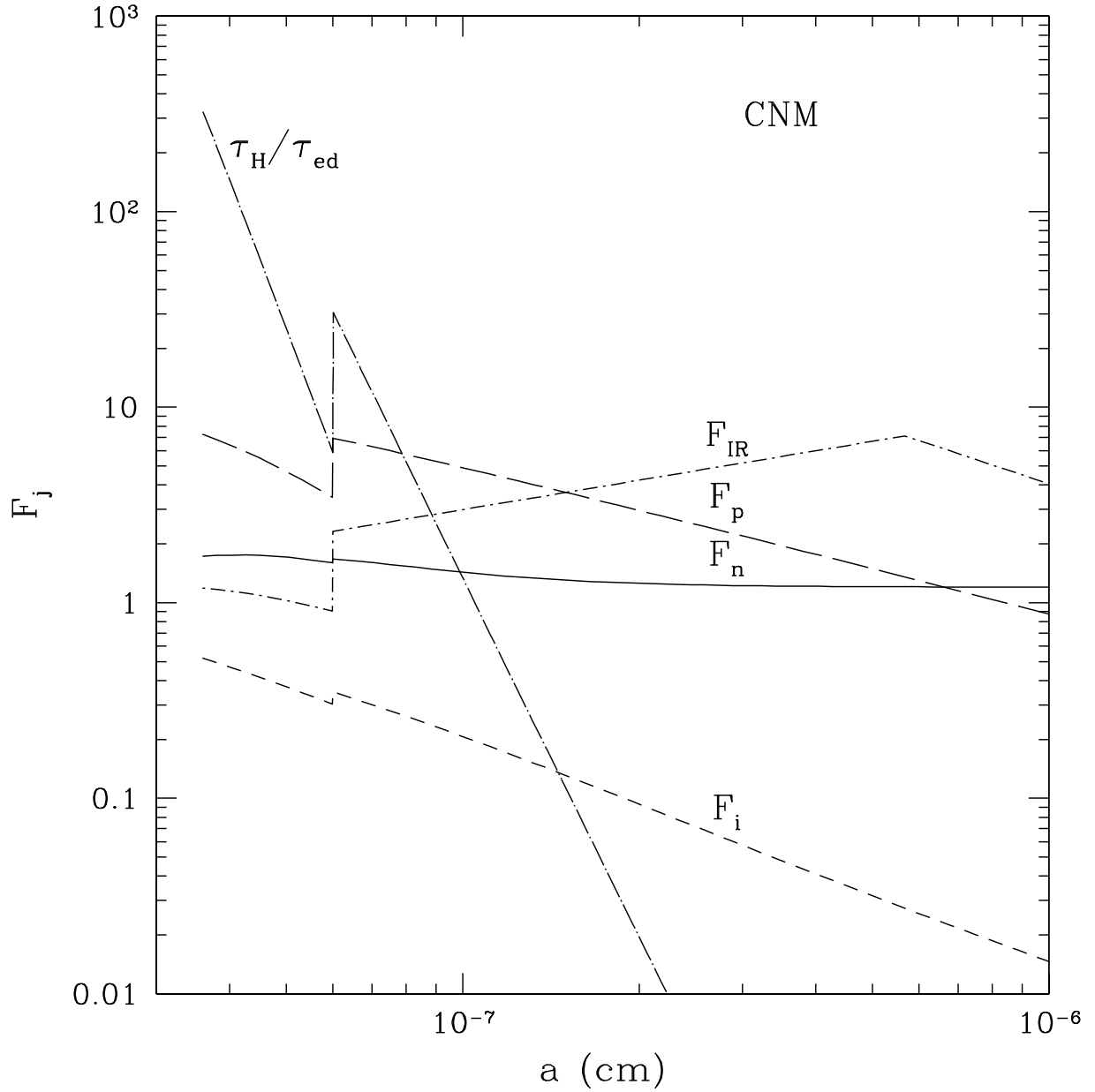


Fig. 5.— Same as Fig. 4 but for “Cold Neutral Medium” conditions. Electric dipole damping dominates for  $a \lesssim 4 \times 10^{-8}$  cm. Plasma drag  $F_p$  is the dominant drag process for  $4 \times 10^{-8} \lesssim a \lesssim 1.5 \times 10^{-7}$  cm. Infrared emission damping is dominant for  $a \gtrsim 1.5 \times 10^{-8}$  cm.

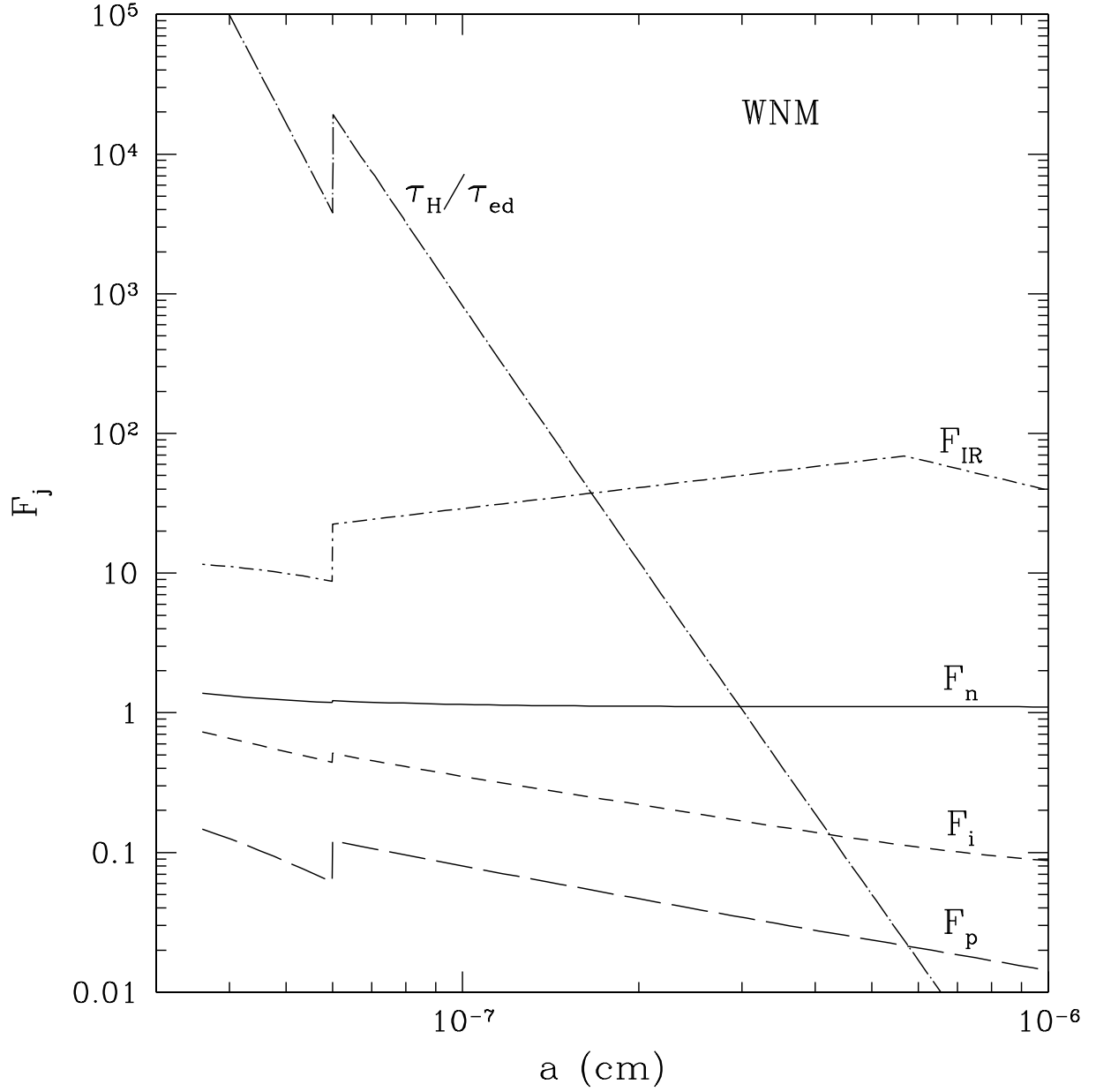


Fig. 6.— Same as Fig. 4 but for “Warm Neutral Medium” conditions. Electric dipole damping dominates for  $a \lesssim 1.5 \times 10^{-8}$  cm, and IR damping dominates for larger grains.

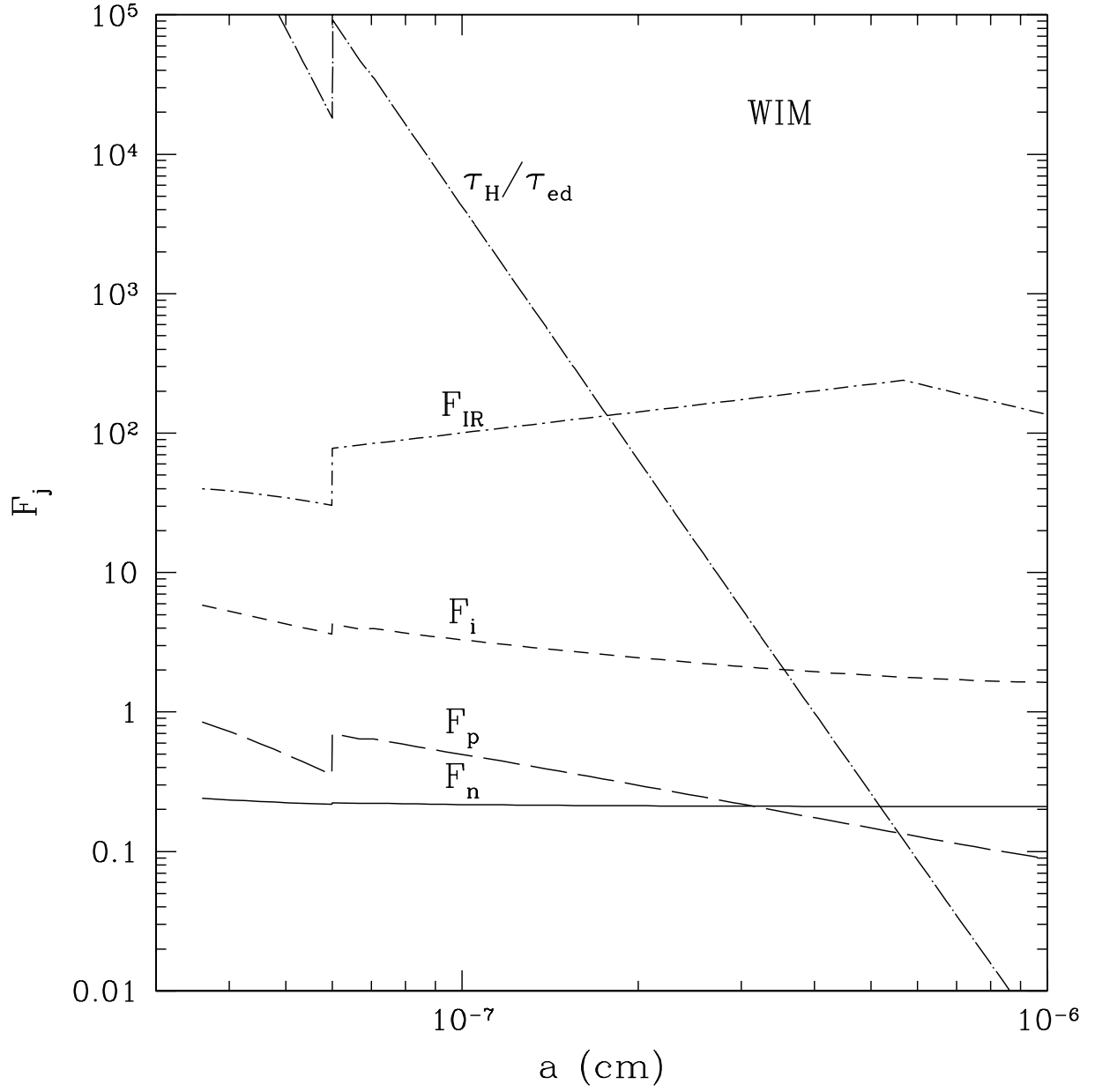


Fig. 7.— Same as Fig. 4 but for “Warm Ionized Medium” conditions.

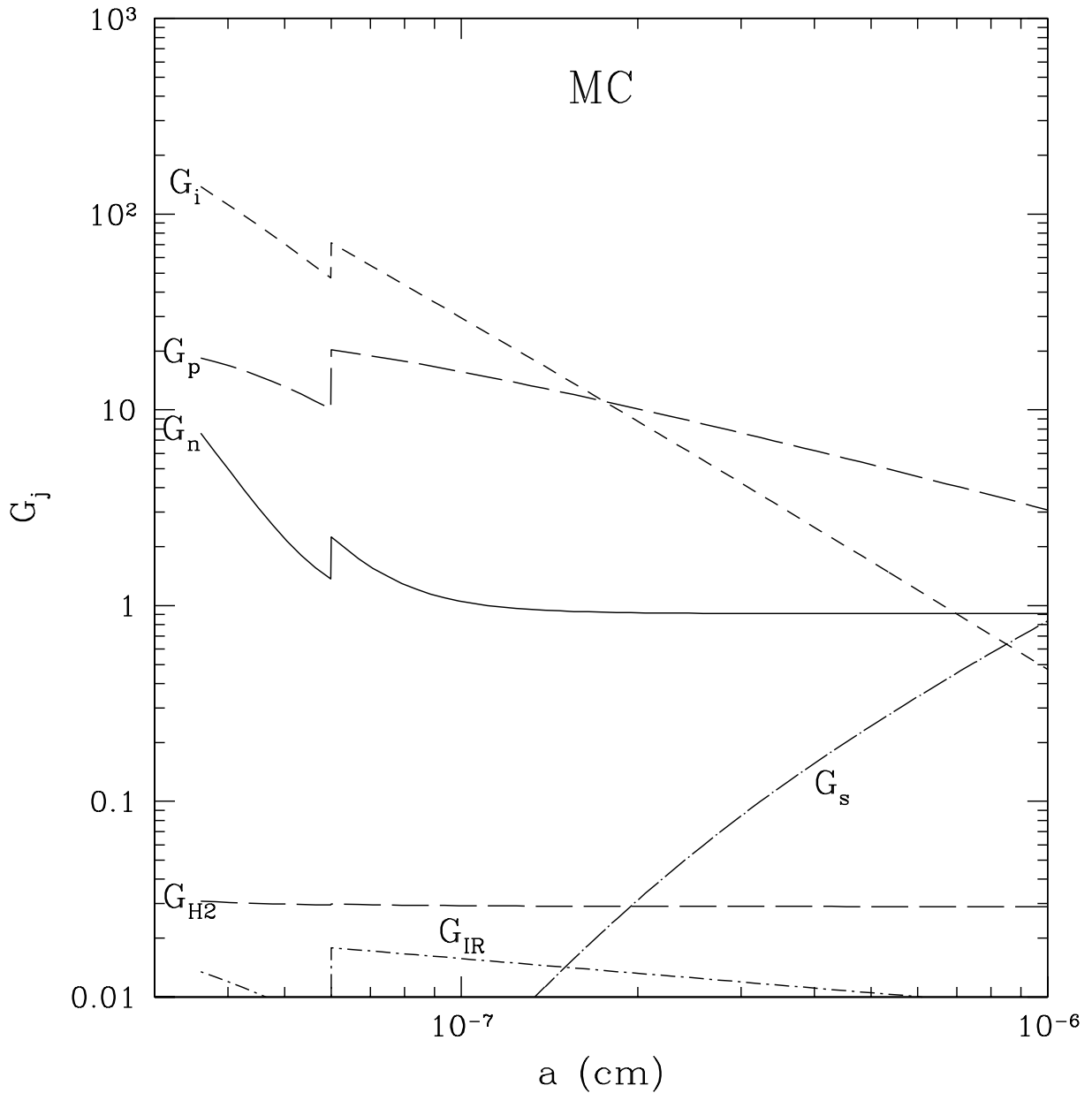


Fig. 8.— Dimensionless rotational excitation functions for neutral collisions [ $G_n$ , eq.(38)], ion collisions [ $G_i$ , eq.(39)-(41)], and plasma drag [ $G_p$ , eq.(43)] for CNM conditions. Ion collisions and plasma drag dominate, despite the low assumed ionization fraction of  $10^{-4}$ . Also shown is the “superthermal” excitation term  $G_s$  for grains with recombination efficiency  $\gamma = 0.1$  and  $N_r$  given by eq.54. Because of the small assumed H fraction (1%)  $H_2$  formation torques are not important in molecular clouds.



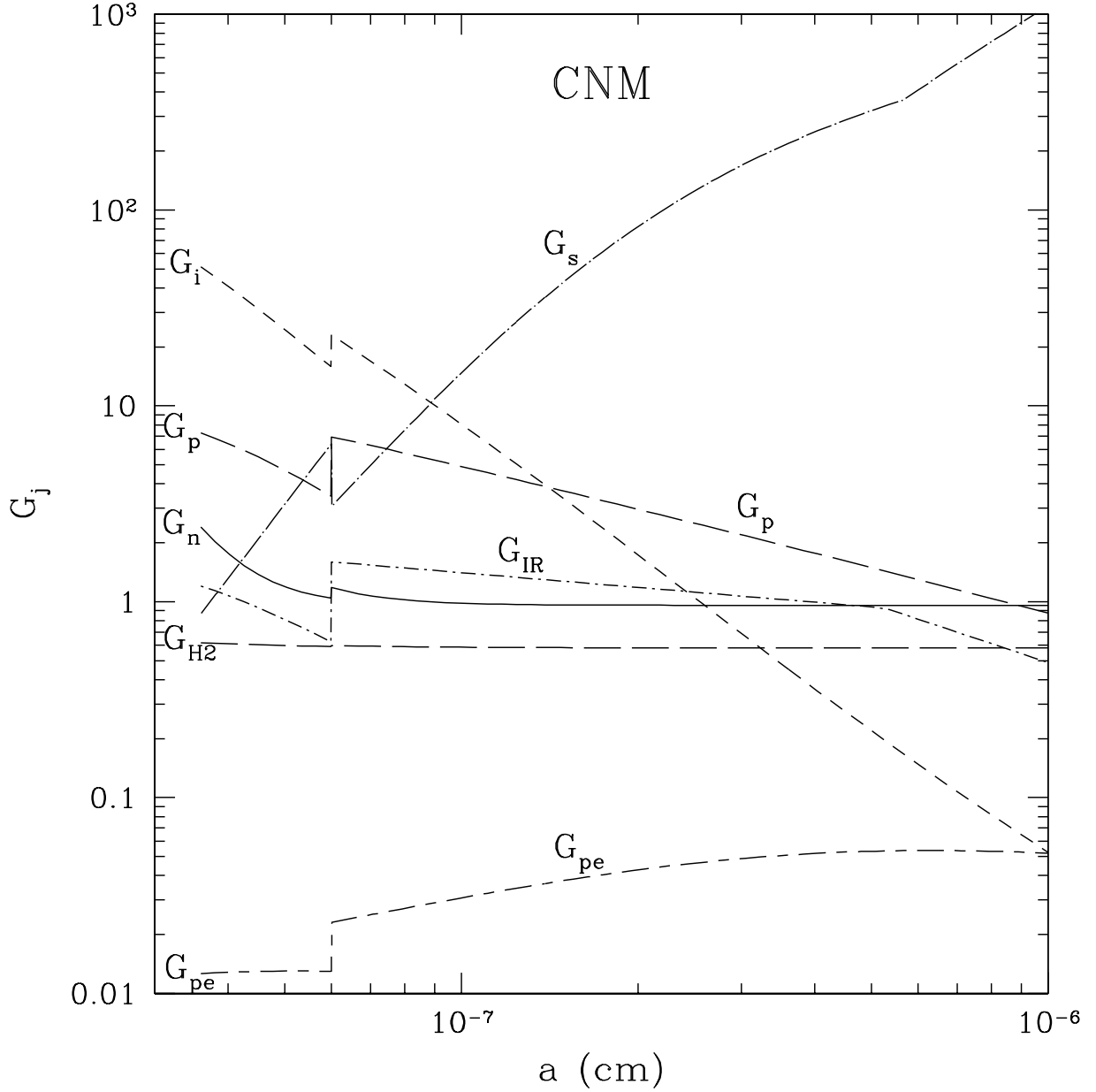


Fig. 9.— Same as Fig. 8 but for CNM conditions. The contribution of infrared emission [ $G_{IR}$ , eq.(44)-(46)] is also shown.  $G_{H2}$  is the contribution if  $H_2$  formation occurs randomly, rather than at preferred sites.  $G_{pe}$  is the contribution from photoelectric emission (eq. 47). Ion collisions and plasma drag dominate for  $a \lesssim 10^{-7}$  cm, and systematic torques from  $H_2$  formation dominate for larger grains for the assumed  $H_2$  formation efficiency  $\gamma = 0.1$ .

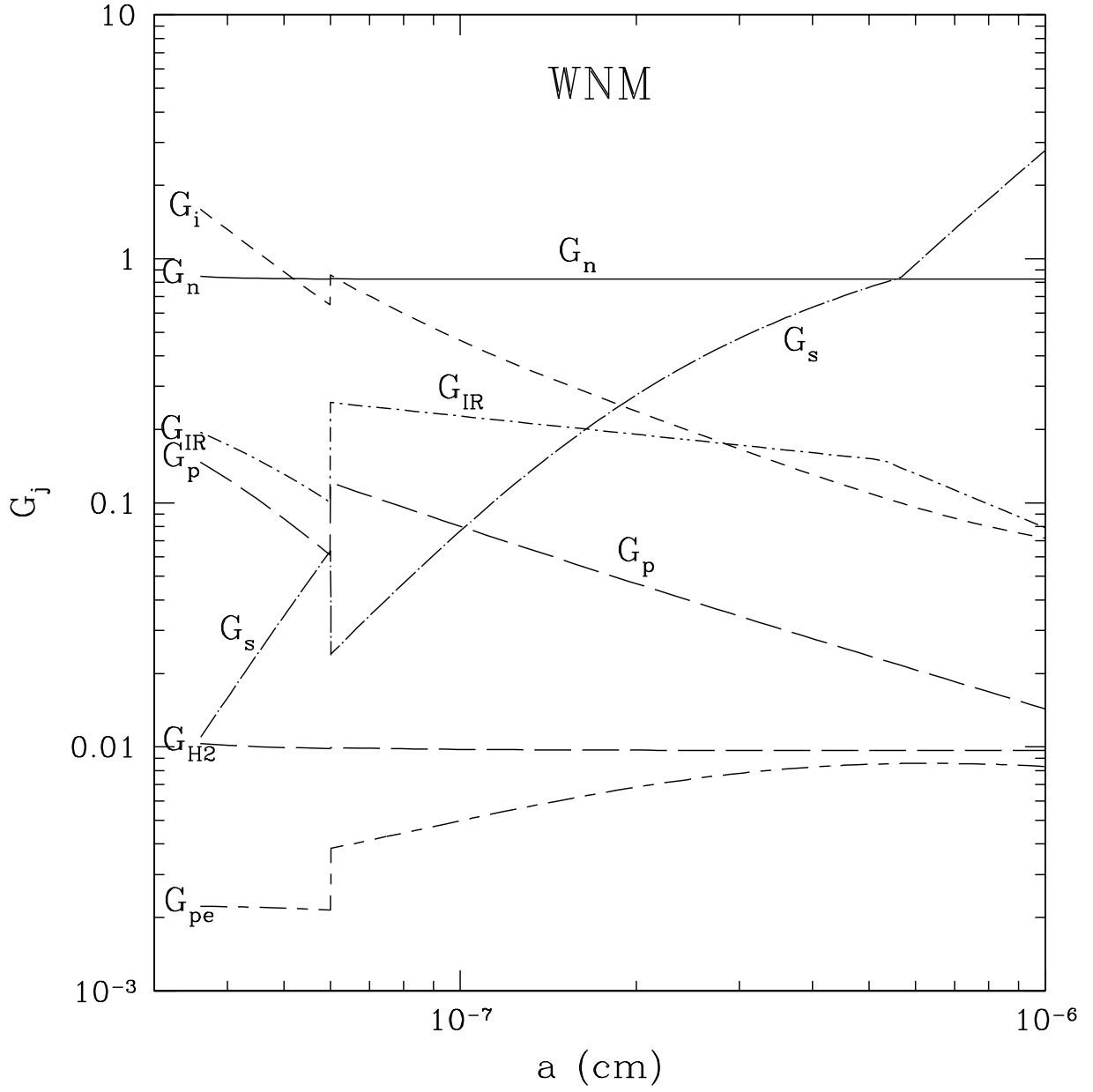


Fig. 10.— Same as Fig. 8 and 9 but for WNM conditions.

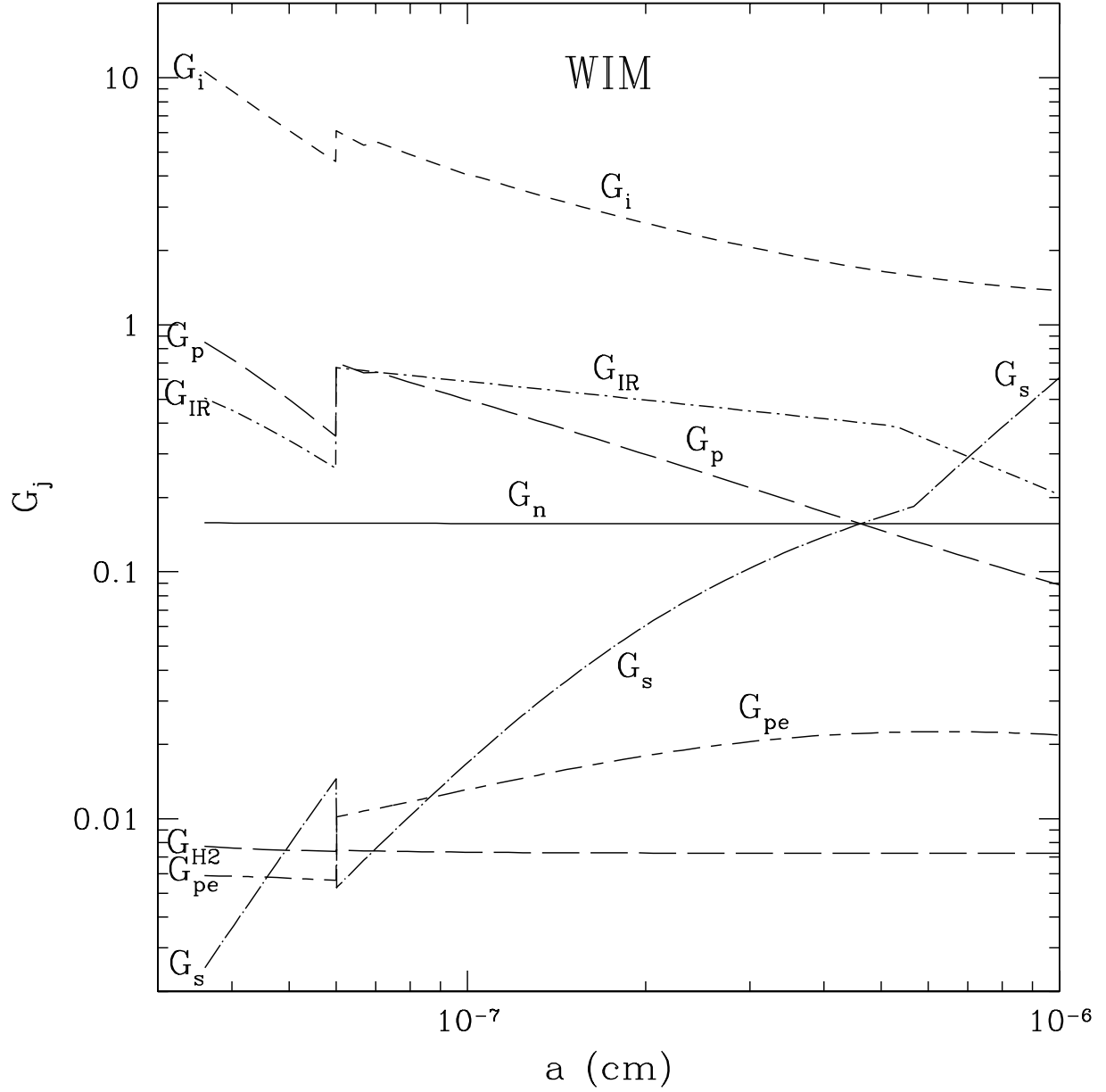


Fig. 11.— Same as Fig. 8 and 9 but for WNM conditions.

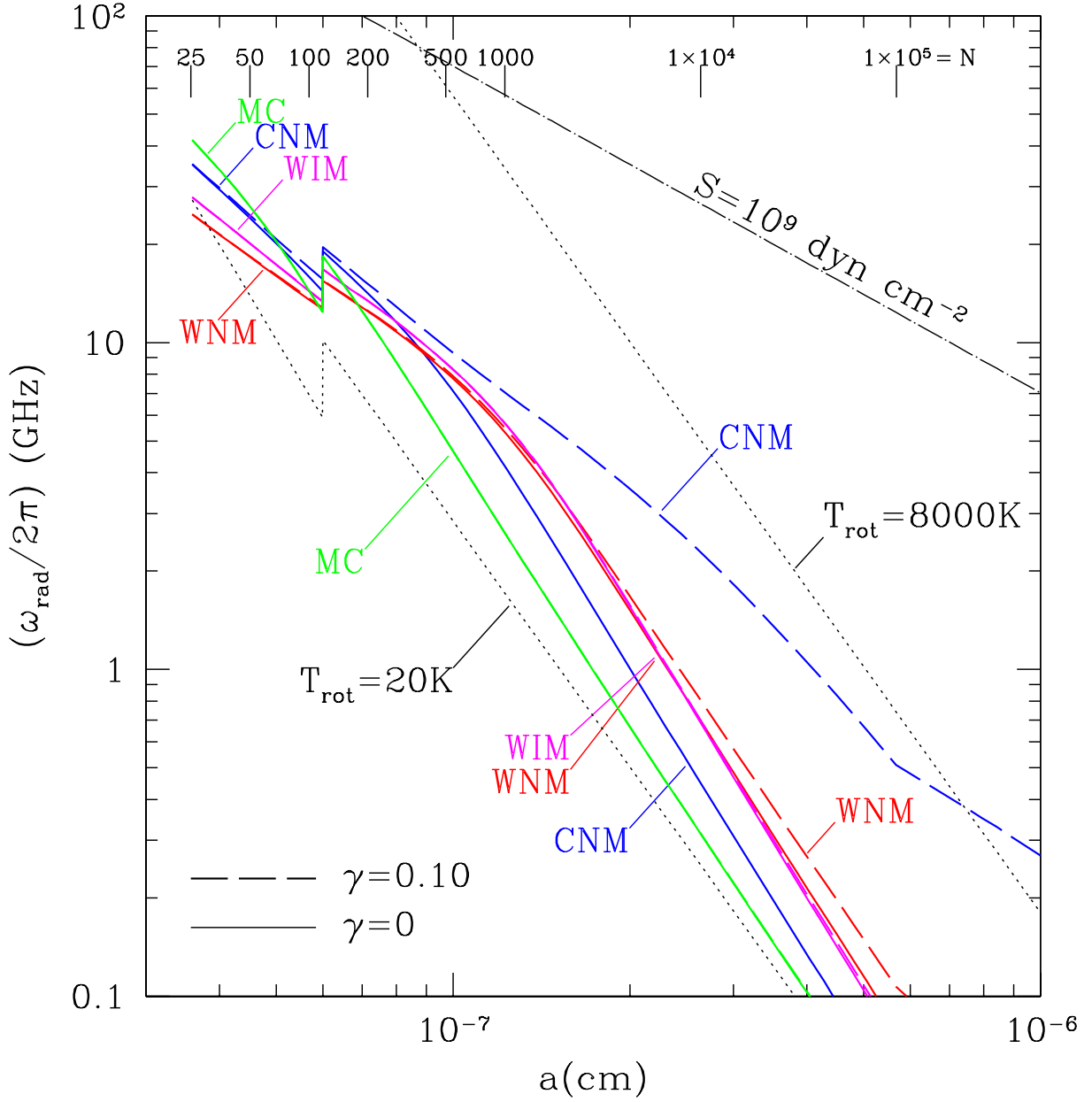


Fig. 12.— Effective rotation rate  $\omega_{\text{rad}} = \langle \omega^4 \rangle^{1/4}$  as a function of grain radius  $a$ , for various environmental conditions, and with and without  $\text{H}_2$  formation. Also shown are the thermal rotation rates [eq. (13)] at  $T = 20\text{K}$  and  $8000\text{K}$ . The number of atoms  $N$  in a grain is indicated at the top of the figure. Also shown is the rotation rate for which the tensile stress equals  $10^9 \text{ dyn cm}^{-2}$ .

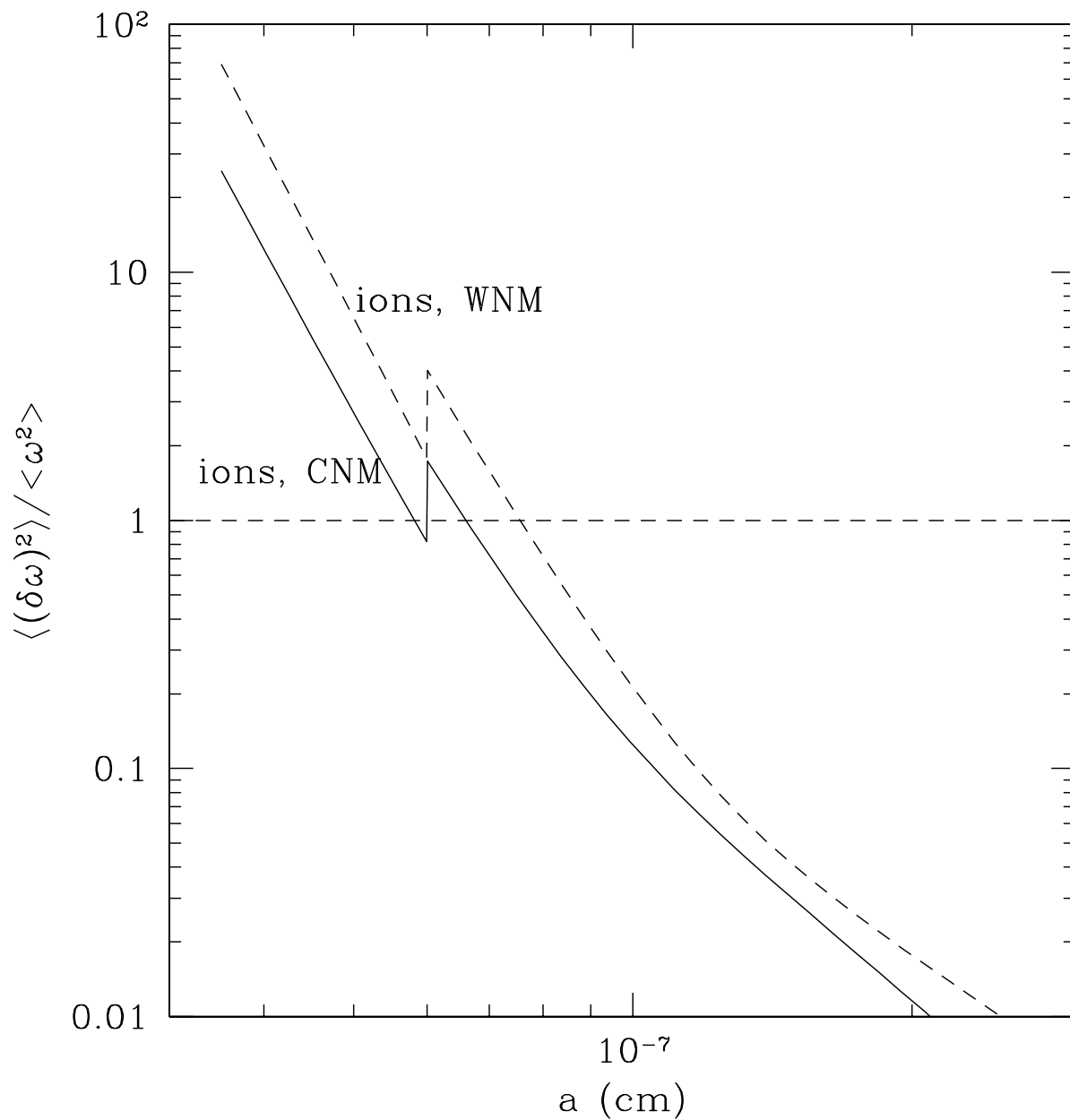


Fig. 13.— Mean square  $\delta\omega$  due to impacting ions relative to mean square  $\omega$  as a function of grain radius  $a$ , under CNM and WNM conditions. It is seen that the rotational excitation process may be treated as continuous for  $a \gtrsim 7 \text{ \AA}$ , but for smaller grains a single ion impact can result in an angular momentum much larger than the time average. For these small grains the angular velocity distribution will depart significantly from a Maxwellian.

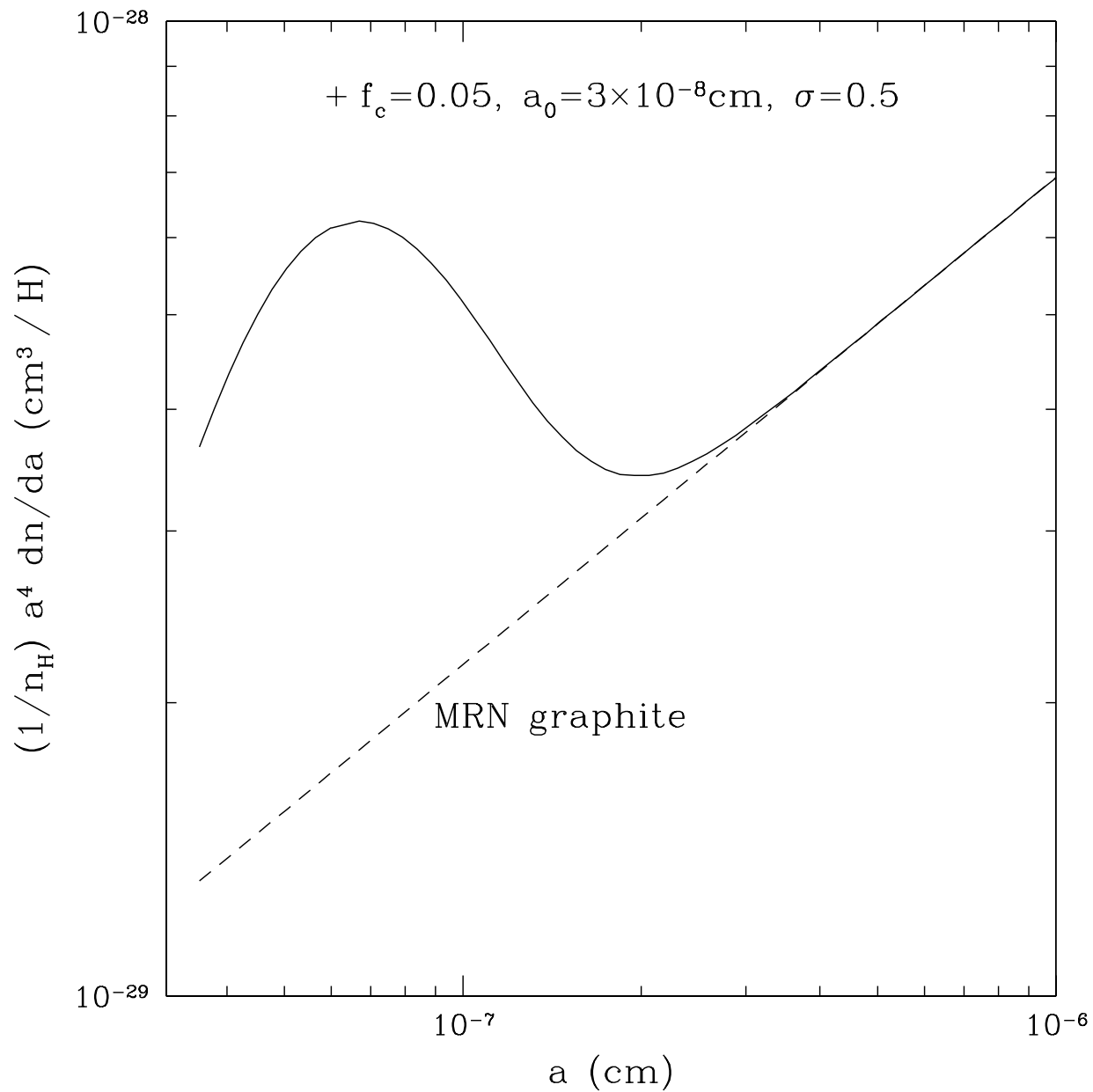


Fig. 14.— Adopted sized distribution for small grains in diffuse regions (CNM, WNM, WIM), with 5% of the total carbon abundance in a log-normal component (see eq. 63). In molecular gas, we assume the number of  $a \lesssim 3 \times 10^{-7} \text{cm}$  grains to be reduced by a factor 5 (see text), so that the log-normal component contains 1% of the carbon.

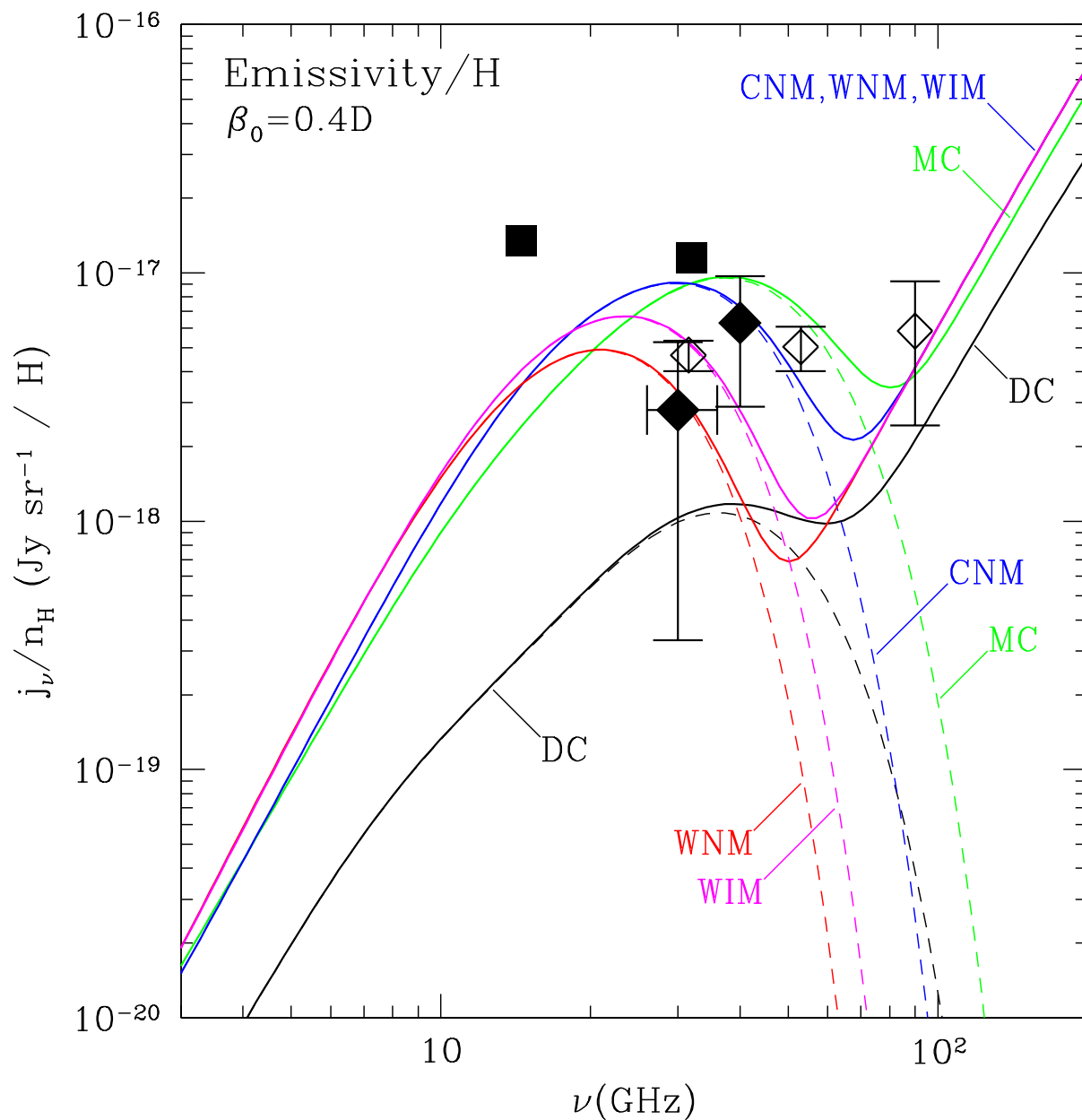


Fig. 15.— Emissivity per H due to ultrasmall spinning dust grains under CNM and WNM conditions, for the size distribution of Fig. 14. Also shown are observed emissivities from *COBE* DMR (open diamonds; Kogut et al. 1996); Saskatoon (filled diamonds; de Oliveira-Costa et al. 1997); and OVRO (filled squares; Leitch et al. 1997).

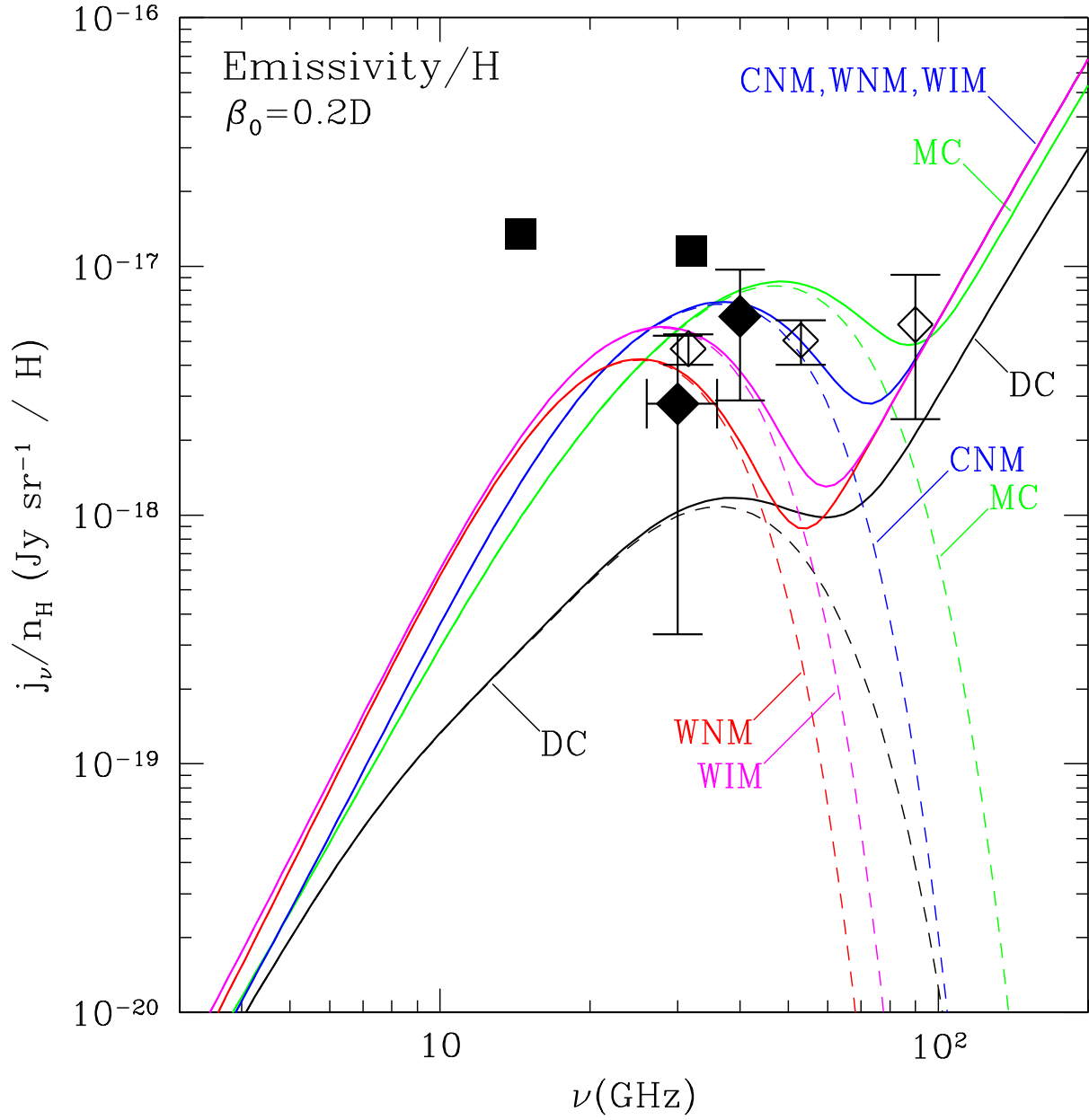


Fig. 16.— Same as Fig. 15 but for intrinsic electric dipole moments  $\mu_i$  reduced by a factor of two ( $\beta_0 = 0.2$  debye).



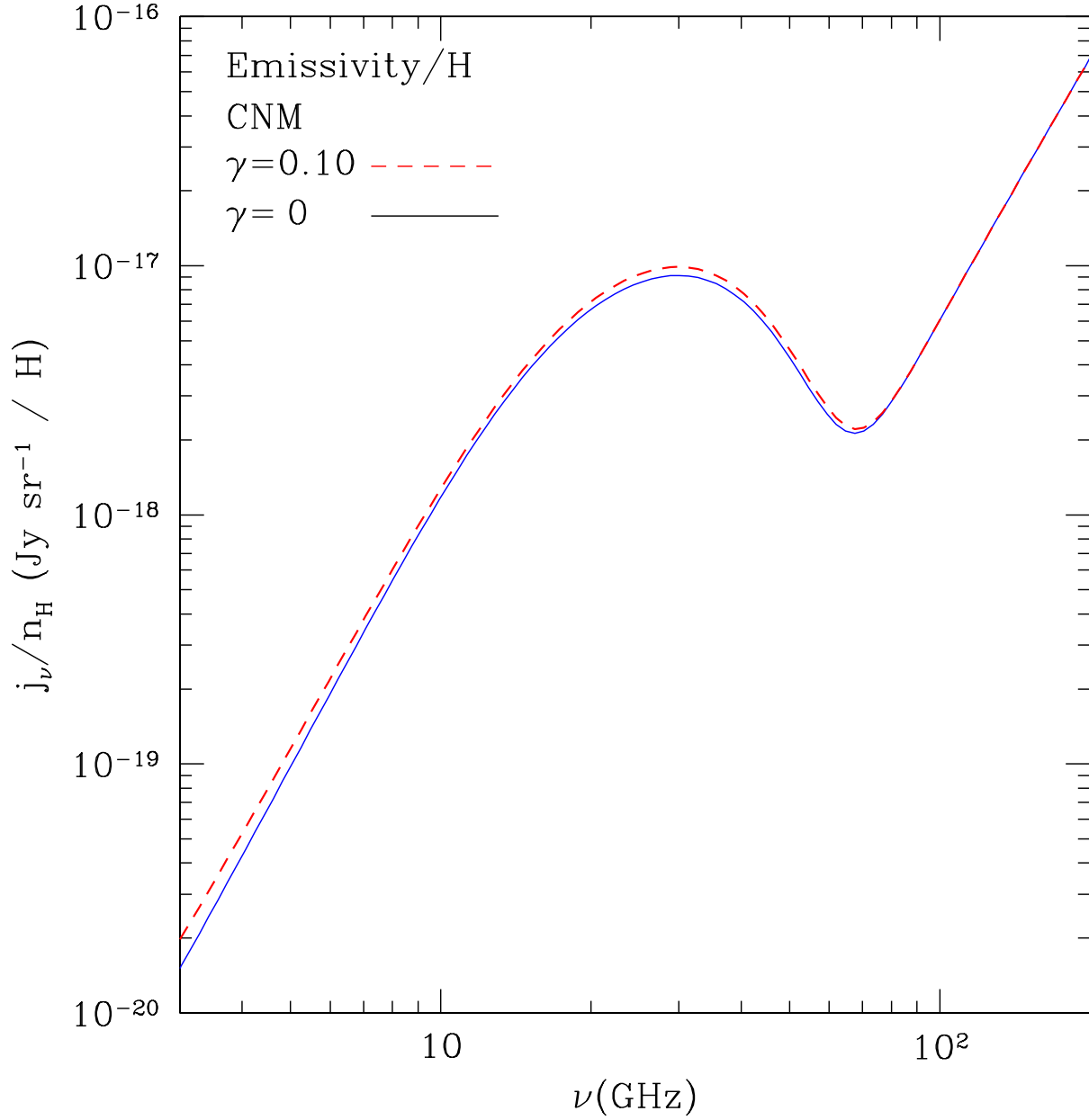


Fig. 17.— Emissivity of CNM grains for  $\gamma = 0$  and  $\gamma = 0.1$ , where  $\gamma$  is the fraction of incident H recombining to form H<sub>2</sub>. The H<sub>2</sub> formation torques have a minimal effect on the emissivity.

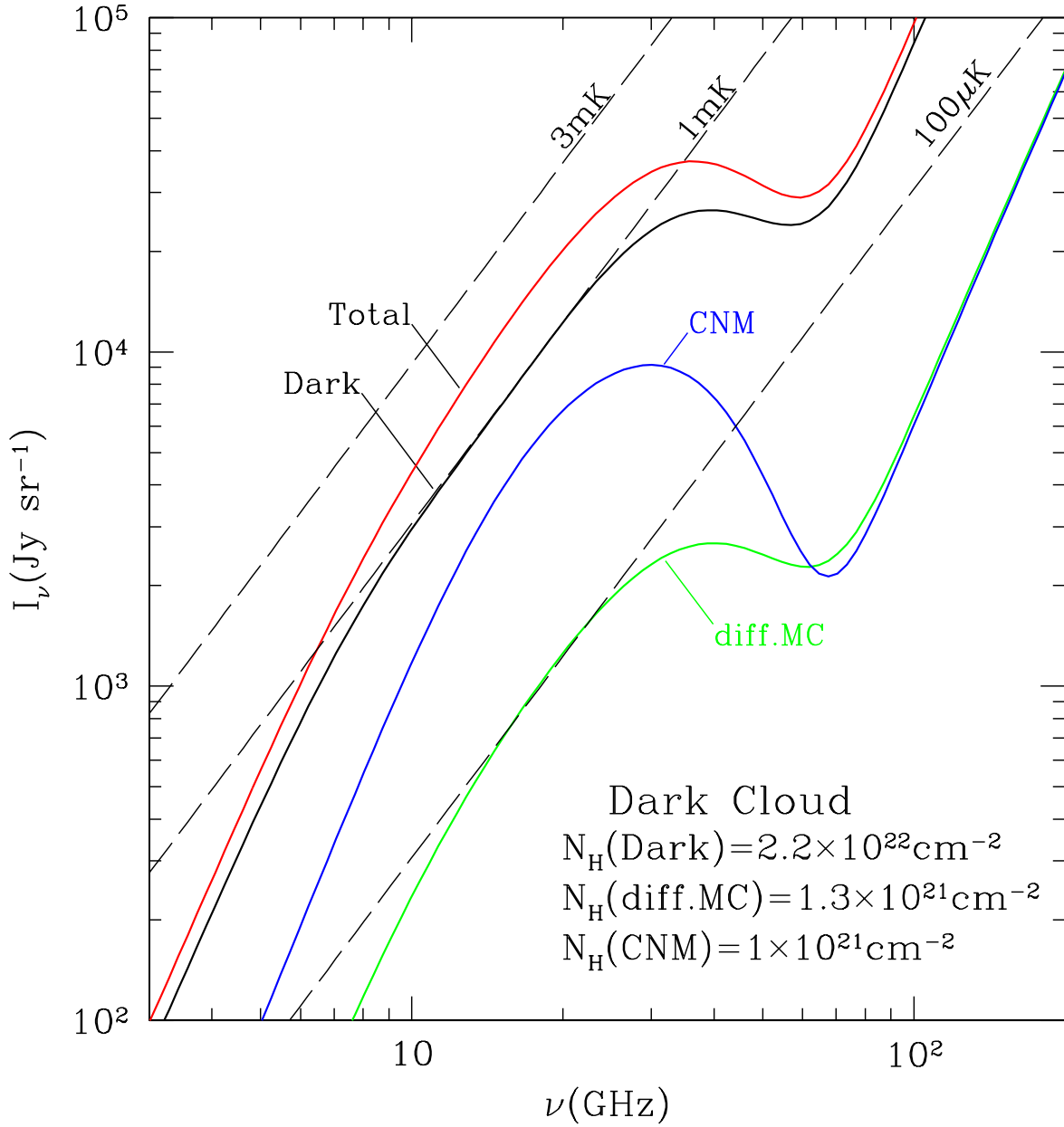


Fig. 18.— The central surface brightness of dust emission from a model cloud resembling L1755 (see text). Dashed lines show antenna temperatures of 100μK and 0.1mK .

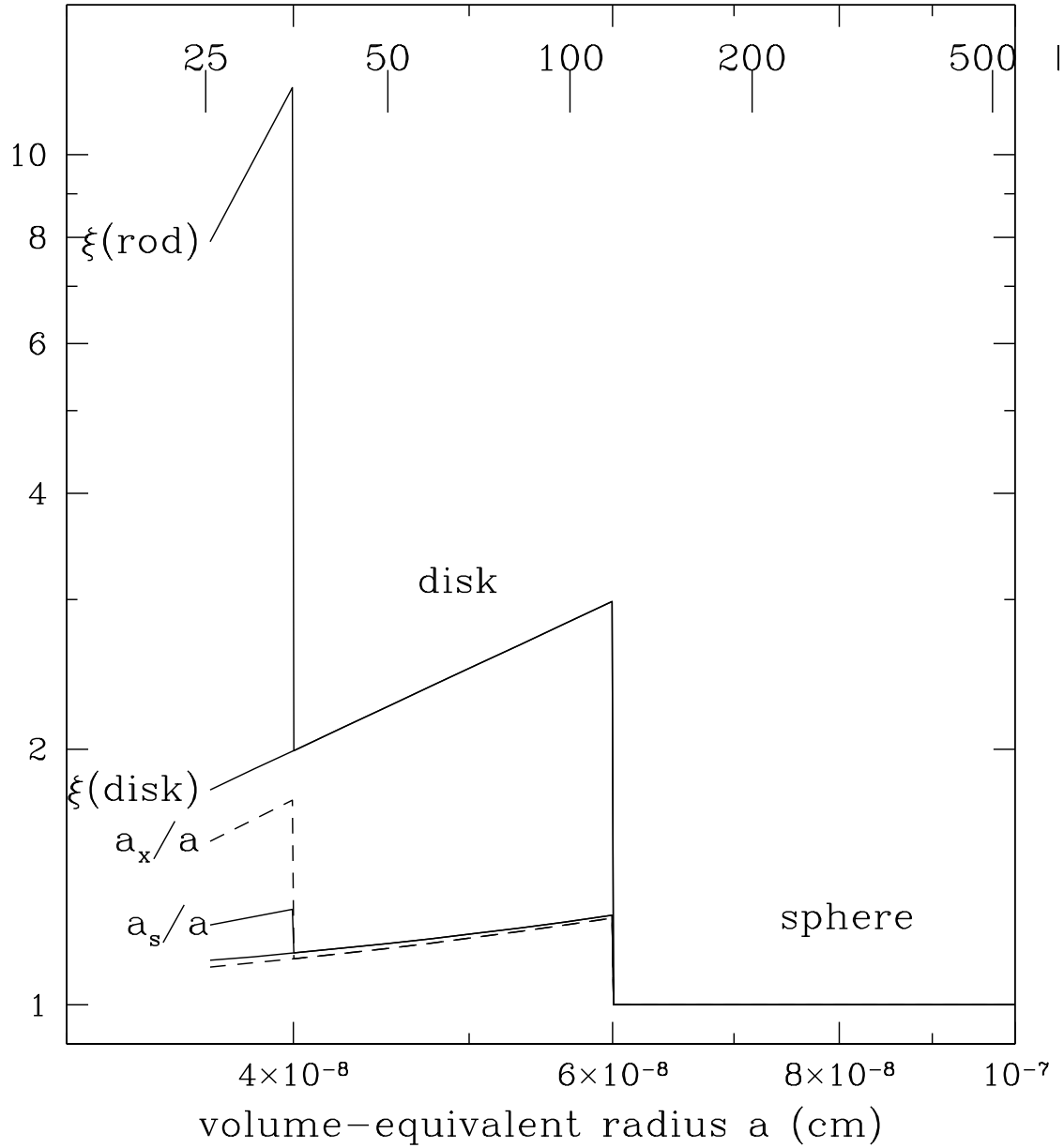


Fig. 19.— The ratios  $a_x/a$  and  $\xi$  as a function of  $a$ . Here  $a$  is the radius of an equal-volume sphere,  $a_x$  is the effective size from eq.(3, and  $\alpha$  is the factor by which the moment of inertia exceeds that of an equal-volume sphere. Tickmarks along the top of the figure show the number of atoms per grain.